

**Correlating Concrete Mix Design to Rheological  
Properties of Fresh Concrete**

**CORRELATING CONCRETE MIX DESIGN TO RHEOLOGICAL  
PROPERTIES OF FRESH CONCRETE**

BY  
OMAR I. DAOUD, B.Sc.

A THESIS  
SUBMITTED TO THE DEPARTMENT OF CIVIL ENGINEERING  
AND THE SCHOOL OF GRADUATE STUDIES  
OF MCMASTER UNIVERSITY  
IN PARTIAL FULFILMENT OF THE REQUIREMENTS  
FOR THE DEGREE OF  
MASTER OF APPLIED SCIENCE

© Copyright by Omar I. Daoud, November 2008

All Rights Reserved

MASTER OF APPLIED SCIENCE (2008)  
(Department of Civil Engineering)

MCMASTER UNIVERSITY  
Hamilton, Ontario

**TITLE:** **Correlating Concrete Mix Design to Rheological  
Properties of Fresh Concrete**

**AUTHOR:** Omar I. Daoud

B.Sc. (Civil Engineering)  
An-Najah National University, Palestine

**SUPERVISOR:** Professor Samir E. Chidiac, Ph.D, P.Eng.

**NUMBER OF PAGES:** xiii, 102

# Abstract

Workability has traditionally been used as one of the measures for controlling concrete mixture proportioning. This metric has provided limits on the water content in the concrete mixture for given aggregate size and type. The slump test, which is commonly used as an assessment of workability, is not adequate for characterizing the flow behaviour / rheology of fresh concrete. Studies have shown that Bingham's rheological properties, namely yield stress and plastic viscosity, provide good description of the flow behaviour of fresh concrete. In this thesis, an experimental program was designed on the basis of factorial design to evaluate the method of Cement Association of Canada for designing and controlling concrete mixture. The variables included in the mix design are water-cement ratio, water content, coarse aggregate size, silica fume, slag and bulk volume of coarse aggregate. In addition, Neuro-Fuzzy network has been adopted to correlate the current mixture proportioning method to the rheological properties of concrete. The network was constructed using experimental data tested in this study. Such correlation allowed the determination of water-cement ratio, water content, fine aggregate and coarse aggregate from compressive strength, yield stress and plastic viscosity.

# Acknowledgements

I would like to express my deep and sincere gratitude to my supervisor Dr. Samir Chidiac for his consistent advice, guidance, encouragement, support and insightful discussions throughout this thesis. This study is part of ongoing research of the concrete rheology group at The McMaster University Centre for Effective Design of Structures under the guidance of Dr. Samir Chidiac. The experimental program included two fellow graduate students, Mr. Fatholla Mahmoodzadeh and Mr. Fayez Moutassem, that I would like to thank for their help and support. My thanks are also extended to Mr. Michael Stolle for his contribution to the experimental program.

I would also like to extend my thanks to the technical staff of the department of Civil Engineering at McMaster University, particularly Kent Wheeler, Dave Perrett and Peter Koudys for their assistance in constructing the moulds and mixing of the concrete.

The financial support of the Natural Sciences and Engineering Research Council of Canada, McMaster University Centre for Effective Design of Structures, and the department of Civil Engineering are gratefully appreciated. I am equally thankful to Lafarge North America Company for the large donation of cement, sand and aggregates as well as to BASF Construction Chemicals for donating the chemical admixtures. Mr. Don Lamb of BASF Construction Chemicals technical advice is also appreciated. I am very grateful to my family for their endless love, support and encouragement through all my life.

# Contents

<b>1</b>	<b>Introduction</b>	<b>1</b>
1.1	Statement of Purpose . . . . .	2
1.2	Overview . . . . .	3
<b>2</b>	<b>Concrete Mixture Proportioning</b>	<b>4</b>
2.1	Design of Concrete Mixture . . . . .	5
2.2	Workability . . . . .	9
2.3	Rheology . . . . .	10
2.4	Measuring Rheological Properties . . . . .	14
2.5	Using Rheology in Concrete Mixture Proportioning . . . . .	18
2.5.1	Pumpability . . . . .	18
2.5.2	Consistency and stability . . . . .	19
<b>3</b>	<b>Experimental Program</b>	<b>21</b>
3.1	Concrete Mix Design . . . . .	22
3.2	Fractional Factorial Design . . . . .	23
3.3	Material . . . . .	26
3.3.1	Aggregates . . . . .	26
3.3.2	Cementitious material . . . . .	29
3.3.3	Air entraining agent . . . . .	29

3.4	Experimental Procedure . . . . .	29
3.4.1	Mixing procedure . . . . .	32
3.4.2	Slump and slump flow . . . . .	32
3.4.3	Density and air content . . . . .	33
3.4.4	Yield stress and plastic viscosity . . . . .	33
3.4.5	Compressive strength test . . . . .	33
<b>4</b>	<b>Experimental Results and Analyses</b>	<b>35</b>
4.1	Results . . . . .	35
4.2	Analysis of Experimental Data . . . . .	43
4.2.1	Slump . . . . .	43
4.2.2	Slump Flow . . . . .	43
4.2.3	Compressive Strength . . . . .	48
4.3	Regression Models . . . . .	48
4.4	Models Validation . . . . .	53
4.5	Models Evaluation . . . . .	56
4.5.1	Slump and Slump flow . . . . .	56
4.5.2	Compressive strength . . . . .	62
4.5.3	Yield stress . . . . .	62
4.5.4	Plastic viscosity . . . . .	64
<b>5</b>	<b>Concrete Mix Design</b>	<b>66</b>
5.1	Neuro-fuzzy model . . . . .	67
5.2	ANFIS Model . . . . .	71
5.2.1	Training the ANFIS model to predict the mix design . . . . .	72
5.2.2	Derived rules for the mix design from the ANFIS model . . . . .	77
5.3	Concrete Mix Design based on the Neuro-Fuzzy method . . . . .	81

<b>6</b>	<b>Conclusions and Recommendations</b>	<b>94</b>
6.1	Recommendations . . . . .	97



# List of Figures

2.1	Concrete mixture proportioning guidelines (F. D. Lydon, 1972) . . . .	6
2.2	Rheological Models (ACI 238, 2008) . . . . .	12
2.3	Shear flow curve - Bingham Model . . . . .	13
2.4	Slump rate machine (SLRM-II) . . . . .	16
2.5	Plastic viscosity and pumping resistance relationship (F. de larrad, 1999)	19
2.6	Equilibrium of fresh concrete under gravity (F. de larrad, 1999) . . . .	20
3.1	14 mm coarse aggregate particle size distribution curve . . . . .	27
3.2	20 mm coarse aggregate particle size distribution curve . . . . .	28
3.3	Fine aggregate particle size distribution curve . . . . .	28
3.4	Slump test of Mix label #41 . . . . .	32
3.5	Pressure vessel used to measure air content . . . . .	33
3.6	Slump Rate Machine (SLRM-II) . . . . .	34
3.7	Tinius Olsen Universal testing machine 600-KN used to test the con- crete 28-day compressive strength . . . . .	34
4.1	Slump-time curve for Mix label #38 . . . . .	41
4.2	Slump-time curve for Mix label #52 . . . . .	41
4.3	Slump-time curve for Mix label #25 . . . . .	42
4.4	Slump-time curve for Mix label #29 . . . . .	42
4.5	Comparison between experimental results and slump flow predicting models . . . . .	47

4.6	Measured slump versus predicted slump (Eq. 4.4) . . . . .	53
4.7	Measured slump flow versus predicted slump flow (Eq. 4.5) . . . . .	54
4.8	Measured compressive strength versus predicted compressive strength (Eq. 4.6) . . . . .	54
4.9	Estimated yield stress (Eq. 2.6) versus predicted yield stress (Eq. 4.7)	55
4.10	Estimated plastic viscosity (Eq. 2.9) versus predicted plastic viscosity (Eq. 4.8) . . . . .	55
4.11	Estimated plastic viscosity (Eq. 2.8) versus predicted plastic viscosity (Eq. 4.9) . . . . .	56
4.12	Water content versus slump measurements . . . . .	57
4.13	Water content versus slump for various levels of w/c; SF=0%, Slag=0%, Size=14mm and CA=0.56 . . . . .	58
4.14	Water content versus slump for various levels of w/c; SF=0%, Slag=0%, Size=20mm and CA=0.63 . . . . .	58
4.15	Measured and computed slump values versus water content for various levels of w/c; SF=0%, Slag=0%, Size=14mm, CA=0.56 and w/c=0.5	59
4.16	Water content versus slump flow measurements . . . . .	60
4.17	Water content versus slump flow for various levels of w/c; SF=0%, Slag=0%, Size=14mm and CA=0.56 . . . . .	61
4.18	Water content versus slump flow for various levels of w/c; SF=0%, Slag=0%, Size=20mm and CA=0.63 . . . . .	61
4.19	w/c versus 28-day compressive strength; SF=0%, Slag=0%, Size=14 mm, CA=0.56 and water content= 199 kg/m <sup>3</sup> . . . . .	63
4.20	Predicted yield stress according to Eq. 2.6 and regression model versus water content for various levels of w/c; SF=0%, Slag=0%, Size=14mm, CA=0.56 and w/c=0.5 . . . . .	63

4.21	Effect of w/c on plastic viscosity for various levels of water; SF=0%, Slag=0%, Size=14mm, CA=0.56 and water content= 199 kg/m <sup>3</sup> . . .	64
4.22	Effect of w/c on yield stress for various levels of water; SF=0%, Slag=0%, Size=14mm, CA=0.56 and water content= 199 kg/m <sup>3</sup> . . . . .	65
5.1	Fuzzy interface system chart (Nayaka et al., 2004, Jang et al., 1993) .	67
5.2	(a) Sugeno fuzzy model, (b) Equivalent ANFIS architecture (Nayaka et al., 2004, Jang et al., 1993) . . . . .	69
5.3	Different membership functions . . . . .	70
5.4	Schematic illustration of the model decision making process . . . . .	72
5.5	General structure of ANFIS model for (a) water-cement ratio; (b) water content; (c) bulk volume of coarse aggregate . . . . .	74
5.6	Degree of membership for (a) Compressive Strength; (b) Yield Stress; (c) Plastic Viscosity - Partitioning to low and high . . . . .	75
5.7	Model prediction versus experimental data for water-cement ratio . .	76
5.8	Model prediction versus experimental data for water content . . . . .	76
5.9	Model prediction versus experimental data for bulk volume of coarse aggregate . . . . .	77
5.10	Guidelines for proportioning concrete mixes using Neuro-Fuzzy method	82
5.11	Design target of compressive strength versus achieved strength using Neuro-Fuzzy method and CAC standard method . . . . .	92
5.12	Design target of slump versus achieved slump using Neuro-Fuzzy method and CAC standard method . . . . .	92
5.13	Design target of yield stress versus achieved yield stress using Neuro-Fuzzy method and CAC standard method . . . . .	93

# List of Tables

2.1	w/c a function of compressive strength (CAC, 2002) . . . . .	7
2.2	Suggested water and air content for different slump and maximum aggregate sizes (CAC, 2002) . . . . .	8
2.3	Bulk volume of coarse aggregate per unit volume of concrete a function of fineness modulus of fine aggregate (CAC, 2002) . . . . .	8
2.4	Recommended levels of workability for various conditions according to the British Standard (F. D. Lydon, 1972) . . . . .	10
2.5	Effect of concrete ingredients on the concrete rheology (ACI 238, 2008)	13
3.1	Variables and corresponding coded values adopted for the experimental program . . . . .	23
3.2	Design of concrete mixtures adopted for this study -Main points . . .	25
3.3	Design of concrete mixtures adopted for this study -Star points . . .	26
3.4	Chemical and physical properties of Hydraulic Cement GU-type 10 and GUb-SF Cement type IP 8 . . . . .	30
3.5	Chemical and physical properties of Ground granulated blast-furnace slag (GGBFS) . . . . .	31
4.1	Slump, slump flow, density, air content and 28-day compressive strength of concrete mixtures -Main points . . . . .	36
4.2	Slump, slump flow, density, air content and 28-day compressive strength of concrete mixtures -Star points . . . . .	37

4.3	Slump, slump flow, slump time, yield stress and plastic viscosity of concrete mixtures obtained using SLRM-II -Main points . . . . .	38
4.4	Slump, slump flow, slump time, yield stress and plastic viscosity of concrete mixtures obtained using SLRM-II -Star points . . . . .	39
4.5	Measured slump according to CAC guidelines versus the measured slump using the traditional slump test and SLRM-II -Main points . .	44
4.6	Measured slump according to CAC guidelines versus the measured slump using the traditional slump test and SLRM-II -Star points . . .	45
4.7	Measured compressive strength according to CAC guidelines versus the measured compressive strength -Main points . . . . .	49
4.8	Measured compressive strength according to CAC guidelines versus the measured compressive strength -Star points . . . . .	50
4.9	Normalizing and model input ranges . . . . .	51
4.10	Coefficients of regression models . . . . .	52
5.1	Coefficients corresponding to w/c, water content and bulk volume of coarse aggregate derived from t-test . . . . .	72
5.2	Rules derived for the water-cement ratio from the results of the network	80
5.3	Rules derived for the water content from the results of the network .	80
5.4	Rules derived for the bulk volume of coarse aggregate from the results of the network . . . . .	80
5.5	Design targets with no mineral admixtures . . . . .	83
5.6	Design targets with mineral admixtures . . . . .	84
5.7	Concrete mixtures following Neuro-Fuzzy method and CAC - mix design with no mineral admixtures . . . . .	86
5.8	Concrete mixtures following Neuro-Fuzzy method and CAC - mix design with mineral admixtures . . . . .	87

5.9	Results of the Neuro-Fuzzy method and CAC - mix design with no mineral admixtures . . . . .	89
5.10	Results of the Neuro-Fuzzy method and CAC - mix design with mineral admixtures . . . . .	90
5.11	Maximum percent difference between calculated values and design values for compressive strength . . . . .	91

# Chapter 1

## Introduction

Workability is one of the measures used to design and control concrete mixture proportioning. Such a metric is employed to control the properties of fresh concrete. Traditionally, the slump test has been used as an assessment of workability. In this context, standard methods for concrete mixture proportioning have established a relation between the slump and concrete proportions (Design and Control of Concrete Mixture, CAC 2002). They postulate that the slump is a function of water content, maximum aggregate size and air entrained. According to ACI committee 238 (2008), workability is defined as "the property of freshly mixed concrete or mortar which determines the ease and homogeneity, with which it can be mixed, placed, consolidated and finished". Other qualitative properties linked to workability are cohesiveness, flowability, compatibility and mouldability (ACI 238, 2008). This quantitative and comprehensive characterization of fresh concrete flow behaviour is needed for workability given that slump measurement is not sufficient. Studies have shown that Bingham's rheological properties, yield stress and plastic viscosity do provide a quantitative measure of the workability of fresh concrete. According to Bingham model, yield stress is a measure of the shear stress required to initiate flow, whereas the plastic viscosity is a measure of the material resistance to flow after the material

begins to flow. Furthermore, it has been reported that slump of fresh concrete correlates very well with yield stress but not with plastic viscosity (Chidiac et al., 2006). This implies that the standard for proportioning concrete mixtures does not account for the plastic viscosity, and therefore is not adequate for characterizing workability as a measure for designing and controlling the quality of fresh concrete mixes. For example, a high slump concrete can be achieved by increasing the amount of water or by adding chemical admixtures. Increasing the amount of water will result in a decrease in the yield stress and plastic viscosity. As a result, problems will arise with the stability and pumpability of the concrete as well as a decrease in the compressive strength and durability of concrete. On the other hand, adding chemical admixtures to the mix while maintaining the same water-cement ratio will yield a decrease in the yield stress and increase in plastic viscosity. Depending on the type of admixtures and quantity, the resultant concrete mixture may become too expensive to pump because of its high plastic viscosity. Also, the addition of water reducers has been shown to lead to an increase in compressive strength and durability. In brief, slump tests which is the current measure of workability can not discriminate between these two concrete mixtures and thus can be misleading as a measure for workability.

## **1.1 Statement of Purpose**

This research aims to evaluate current Canadian design method of concrete mixture proportioning and slump test for controlling the quality of fresh concrete. Bingham's rheological properties, namely yield stress and plastic viscosity are also evaluated for the purpose of characterizing the flow behaviour of fresh concrete and ultimately workability. Experimental program was derived from the factorial design method and includes the following variables: water-cement ratio, water content, coarse aggregate size, percent addition of silica fume, percent addition of slag and bulk volume of coarse



aggregate. The aim is to incorporate the rheological properties of fresh concrete in the design and control of concrete mixtures.

## 1.2 Overview

This thesis contains six chapters, First chapter presents an introduction to the thesis and a corresponding statement of purpose. Chapter two provides a review of design and control of concrete mixtures. Rheology of fresh concrete including test methods and mathematical models are also briefly presented. The potential benefit of employing the rheology in characterizing the behaviour of fresh concrete are discussed.

Chapter three presents the experimental program developed on the basis of factorial design to study the effect of water-cement ratio, water content, coarse aggregate size, percent addition of silica fume and slag and the bulk volume of coarse aggregate on the slump, slump flow, slump rate, yield stress, plastic viscosity and compressive strength.

Chapter four presents the results of the experimental program conducted in Chapter three. Comparison between the design values and measured values of slump and compressive strength are conducted. Regression models were derived for slump, slump flow, yield stress, plastic viscosity and compressive strength.

Chapter five defines the Neuro-Fuzzy technique and presents it as a useful method to correlate the current mix design to the rheological properties of fresh concrete and compressive strength. Rules were derived for calculating the mixture proportions from the strength, yield stress and plastic viscosity on the basis of the network results. The accuracy of such rules in proportioning concrete mixture were evaluated.

Finally, the conclusions and recommendations of this research are drawn in Chapter six.

## Chapter 2

# Concrete Mixture Proportioning

Concrete is a mixture of water and solid particles which typically range in size between 20 mm and  $1\mu m$  (Tattersall and Banfill, 1983). This heterogeneous composition of concrete has been shown to affect its flow behavior as well as its mechanical, physical and durability properties. Accordingly, research has been carried out for determining the content of each proportion in the concrete mixture. Such a mixture needs to possess the desired properties for workability, strength and durability while remaining economical (F. D. Lydon, 1972).

This chapter contains five sections. First section presents an introduction to the concrete mixture proportioning and the basis for its design. In Section two, the definition of workability is reviewed along with the use of workability measures for controlling the quality of concrete mixture proportioning. Rheology is defined in Section three, which also includes a review of the rheological models proposed for fresh concrete. Description of the apparatus used to measure the rheological properties of fresh concrete is presented in Section four. The relevance of the rheological properties for describing and controlling the flow of fresh concrete, particularly, the flowability, pumpability and stability, is discussed in Section five.

## 2.1 Design of Concrete Mixture

Concrete mixture proportioning provides a recipe for manufacturing concrete. It is a process that has been developed for determining the concrete ingredients with specified characteristics, using local materials (Design and Control of Concrete Mixture, CAC 2002). Prior to 1918, most theories of concrete mixture proportioning were developed on the assumption that maximum density leads to the greatest strength and imperviousness of concrete (ACI Proportioning Concrete Mixes, 1974). According to ACI Proportioning Concrete Standards (ACI Proportioning Concrete Mixes, 1974), these theories include, Arbitrary assignment (1:2:4), Void ratio, Maximum density, Fineness modulus, Surface area of aggregate, Cement content, and Water-cement ratio. In 1918, Abrams reported that the water-cement ratio is the most critical parameter for designing concrete proportions (ACI Proportioning Concrete Mixes, 1974). In 1944, the “first American Concrete Institute (ACI) standard method for proportioning concrete mixture” was produced, and it was based on the water-cement-ratio methodology put forward by Abrams. Moreover, the first standardized method also used the slump test, which was developed by Abrams, as a measure of workability (ACI Proportioning Concrete Mixes, 1974). The test was used to measure the aggregate-cement ratio in the mixture.

In 1954, two new concepts were added to the ACI standard method, air entrainment and ratio of unit volume of dry rodded coarse aggregate to volume of coarse aggregate. The second concept was used to estimate the coarse aggregate content in the mixture. Subsequently, the specific gravity factor was introduced to the proportioning standard in order to determine the absolute volume for each ingredient in the mixture. The specific gravity factor is defined as the ratio of the material weight to the effective volume displaced by it (ACI Proportioning Concrete Mixes,



is then determined following the guidelines given in Table 2.2. The suggested water content is for crushed angular coarse aggregate and needs to be adjusted for aggregate with other shape and texture. This permits the determination of the cement content. The volume of coarse aggregate per unit volume of concrete is determined from the maximum coarse aggregate size and fineness modulus of fine aggregate as given in Table 2.3.

Table 2.1: w/c a function of compressive strength (CAC, 2002)

Compressive strength after 28 days, MPa	Water-cementing materials ratio by mass	
	Non-air-entrained concrete	Air-entrained concrete
45	0.38	0.3
40	0.42	0.34
35	0.47	0.39
30	0.54	0.45
25	0.61	0.52
20	0.69	0.6
15	0.79	0.7

The remaining ingredient is the fine aggregate content, which is estimated using the volume method. This method involves calculating the weights of water, cement and coarse aggregate, which are then converted to volume. By subtracting the sum from the total concrete mixture volume, the volume of fine aggregate is obtained. Then, the calculated volume is converted to weight (ACI Proportioning Concrete Mixes, 1974). This method, therefore, requires a priori determination of the specific gravity factor for all the concrete ingredients. It should be noted that the volume of air content in the mixture is also considered in the volume method.

Table 2.2: Suggested water and air content for different slump and maximum aggregate sizes (CAC, 2002)

Slump (mm)	Water, kilograms per cubic metre of concrete							
	10 mm	14 mm	20 mm	28 mm	40 mm	56 mm	80 mm	150 mm
<b>Non-air entrained concrete</b>								
25 to 50	207	199	190	179	166	154	130	113
75 to 100	228	216	205	193	181	169	145	124
150 to 175	243	228	216	202	190	178	160	-
Approximate amount of entrapped air in non-air entrained concrete (%)	3	2.5	2	1.5	1	0.5	0.3	0.2
<b>Air-entrained concrete</b>								
25 to 50	181	175	168	160	150	142	122	107
75 to 100	202	193	184	175	165	157	133	119
150 to 175	216	205	197	184	174	166	154	-
CSA A23.1 Recommended total air content (%)								
Category 1	6 to 9	5 to 8		4 to 7	-	-	-	-
Category 2	5 to 8	4 to 7		3 to 6	-	-	-	-

Table 2.3: Bulk volume of coarse aggregate per unit volume of concrete a function of fineness modulus of fine aggregate (CAC, 2002)

Nominal maximum size of aggregate (mm)	Bulk volume of dry-rodded coarse aggregate per unit volume of concrete for different fineness moduli of fine aggregate			
	2.4	2.6	2.8	3
10	0.5	0.48	0.46	0.44
14	0.59	0.57	0.55	0.53
20	0.66	0.64	0.62	0.6
28	0.71	0.69	0.67	0.65
40	0.75	0.73	0.71	0.69
56	0.78	0.76	0.74	0.72
80	0.82	0.8	0.78	0.76
150	0.87	0.85	0.83	0.81

## 2.2 Workability

The term workability has received many interpretations. According to the American Concrete Institute (ACI), workability is defined as “the property of freshly mixed concrete or mortar which determines the ease and homogeneity, with which it can be mixed, placed, consolidated and finished” (ACI 238, 2008). CAC (2002) defines workability as “the ease of placing, consolidating and finishing freshly mixed concrete” (Design and Control of Concrete Mixture, CAC 2002). On the other hand, the Japanese Association of Concrete Engineers defines workability as “that property of freshly mixed concrete or mortar which determines the ease with which it can be mixed, placed and compacted due to its consistency, the homogeneity with which be made into concrete and the degree with which it can resist separation of materials” (C. F. Ferraris, 1999). These definitions indicate that workability encompasses cohesiveness and consistency. Cohesiveness is defined for concrete as “the ease of trowelling and visual judgment of resistance to segregation” (Mehta et al., 1993), and consistency as “the relative mobility or ability of fresh concrete or mortar to flow” (ACI 238, 2008). These terms, in addition to flowability, finishability and pumpability, provide a qualitative description of concrete workability.

Numerous test methods have been developed to quantitatively measure the workability of fresh concrete. The slump test, developed in 1941, has remained the test of choice for many standards because of its ease-of-use and low cost. Other tests such as Compacting factor test (British Standards 1881), Vebe test BS 1881 (British Standards 1881), and Flow table test (DIN 1048) have also been proposed to measure workability.

Workability is also used to control the quality of concrete. Therefore it serves two purposes; the design of concrete to meet job conditions and to control the quality of fresh concrete. The challenge remains how to choose a suitable workability for each

circumstances, then convert it to a quantitative term which could act as a design target of the mixture design. For instance, the British Standard (British Standards Institution, Methods of Testing Fresh Concrete 1970) has categorized workability into 4 levels; high, medium, low and very low, and used the Slump test, Compacting factor test and V-B Consistometer test to quantify workability. Table 2.4 provides a summary of the recommended levels of workability for some conditions (F. D. Lydon, 1972). Research has shown that these tests are not sufficient to quantify the workability of fresh concrete and that rheology is the best approach to achieve such characterization (Tattersall and Banfill, 1983).

Table 2.4: Recommended levels of workability for various conditions according to the British Standard (F. D. Lydon, 1972)

<b>Workability</b>	<b>Suitable use</b>	<b>Compacting Factor</b>	<b>Slump range (mm)</b>	<b>V-B range</b>
Very low	Section with access to vibration	0.78	0	15-30
Low	Simply reinforced section vibrated	0.85	0-50	8-12
Medium	More congested section vibrated	0.92		3-5
High	Heavily reinforced section vibrated	0.95	50-100	1-3

## 2.3 Rheology

Rheology is defined as “the science of the deformation and flow of matter, which is concerned with relation between stress, rate of strain and time” (Tattersall and Banfill, 1983). In the field of concrete, rheology is needed to characterize workability.



In order to achieve such an objective, an understanding of the material flow behaviour is merited.

Many rheological models have been developed to describe the flow of liquids or liquids with solid suspensions (Tattersall and Banfill, 1983). The variations among these models are their description of the onset of flow and the flow behaviour. Materials start to flow when the shear stress exceeds a threshold limit referred to as yield stress. For some materials, such as water and oil, the yield stress is equal to zero and for others, such as fresh concrete, it is greater than zero. There are three basic models that have been used to describe the flow behaviour of liquids or liquids with solid suspensions, namely Newtonian, Power and Bingham. ACI 238 (2008) has defined mathematical notations for these models and the corresponding mathematical model is given below:

Newtonian law

$$\tau = \eta \dot{\gamma} \quad (2.1)$$

Power law

$$\tau = \kappa \dot{\gamma}^n \quad (2.2)$$

Bingham

$$\tau = \tau_o + \eta \dot{\gamma} \quad (2.3)$$

Where  $\tau_o$  is the yield stress (Pa),  $\eta$  the plastic viscosity (Pa.s),  $\dot{\gamma}$  the shear rate ( $s^{-1}$ ),  $\kappa$  the consistency, and  $n$  the Power index representing the deviation from the newtonian behavior viscosity. It should be noted that when  $n=1$ , the power law model provides a description of the Newtonian fluid, and when  $n$  is greater than 1 or less than 1, the model represents shear thickening and shear thinning behaviour, respectively. For normal slump concrete, research has shown that the Bingham model provides a good description of the flow. However, for high slump concrete, referred

to as self consolidating concrete, it has been found that the flow is non-newtonian and is best described using Herschel-Bulkley model given by:

$$\tau = \tau_o + \kappa \dot{\gamma}^n \quad (2.4)$$

Figure 2.2 illustrates the shear stress and strain rate relation for the above noted models.

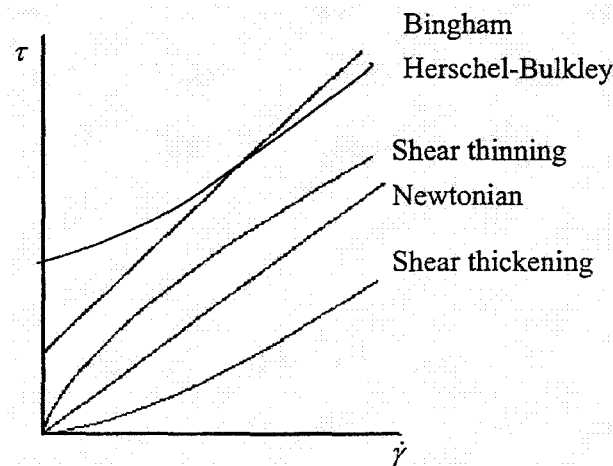


Figure 2.2: Rheological Models (ACI 238, 2008)

Bingham model defines the shear flow curve as a linear relationship between the shear rate and shear stress. Such relationship is represented by the yield stress as a y-intercept and the plastic viscosity as a slope as shown in Figure 2.3. In this context, two rheological properties are needed to characterize the flow; yield stress and plastic viscosity.

Yield stress is “a critical shear stress value below which an ideal plastic or viscoplastic material behaves like a solid. Once the yield stress is exceeded, a plastic material yields while a viscoplastic material flows like a liquid” (ACI 238, 2008). Effects of concrete ingredients on yield stress values are summarized in Table 2.5.

Plastic viscosity is a material property which measures the resistance to a change in shape or arrangement of its constituents (Chidiac et al., 2003). In a mathematical

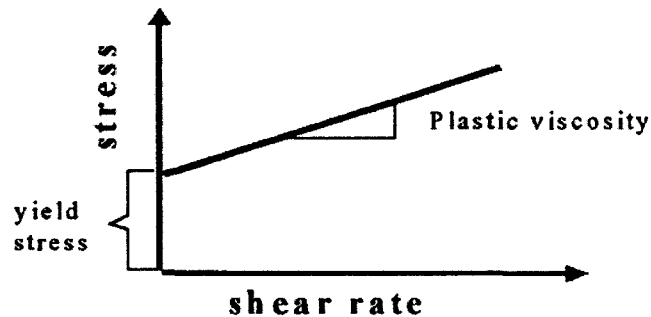


Figure 2.3: Shear flow curve - Bingham Model

sense, plastic viscosity is “the excess of the shear stress over the yield stress divided by the shear rate and equal to differential viscosity” (ACI 238, 2008). The effects of concrete ingredients on the plastic viscosity are also summarized in Table 2.5. These results indicate that the rheological properties are sensitive to the proportions of concrete ingredients.

Table 2.5: Effect of concrete ingredients on the concrete rheology (ACI 238, 2008)

<b>Factors</b>	<b>Yield stress</b>	<b>Plastic viscosity</b>
Cement content	Decrease	Decrease
Water content	Decrease	Decrease
Aggregate volume fraction	Increase	Increase
Sand to aggregate ratio	Optimum value	Optimum value
Microfines content	Mixed	Mixed
Water-reducing admixtures	Decrease	Mixed
Air-entrainment agent	Mixed	Decrease
Viscosity modifying admixtures	Increase	Increase
Fly ash	Decrease	Mixed
Silica fume (Low dosage)	Decrease	Decrease
Silica fume (High dosage)	Increase	Increase
Slag (GGBFS)	Mixed	Increase

## 2.4 Measuring Rheological Properties

Testing methods for measuring workability have been categorized as single point test or multipoint test (ACI 238, 2008). A single point test refers to a single point on the shear flow curve, such as the slump test which provide a measure of yield stress (Chidiac et al., 2006). While, a multipoint test refers to many points on the shear flow curve, thus affording a description of the flow. These tests are carried out using concrete rheometers.

The flow properties of fresh concrete in a single point test are handled by assuming a constant shear rate for the shear flow (Tattersall and Banfill, 1983). This assumption provides an incomplete description of the fresh concrete behavior. However, single point apparatuses have been used because they are simple and easy to use. Examples of these apparatuses are the Compaction Factor test, V-B Consistometer test, Free Orimet test, Kelly Ball test and Slump test. Refer to ACI 238 (2008) for a comprehensive list and assessment of these tests.

Slump test is a simple test employed to evaluate the workability of concrete. It is widely used since it is simple, inexpensive and can be carried out in the field with very little training. The slump test is based on measuring how much concrete, which has been placed in a standard mould, slumps after removing the mould. The resulting single point in this test is the slump value which has been correlated to the yield stress (Chidiac et al., 2006). However, the slump test is characterized by subjectivity. In other words, its result depends on the dimensions and detailed arrangement of apparatus as well as the technique of performing such a test (Tattersall and Banfill, 1983). Additionally, the slump test can not be used for concrete with very low or high workability.

Multipoint test characterizes the flow properties by varying the shear rate in order to measure more stresses on the shear flow curve. The rheological properties, yield

stress and plastic viscosity, are estimated in the multipoint test by assuming that the flow obeys Bingham model or Herschel-Bulkley model. Many apparatuses have been developed to measure the flow of fresh concrete. Examples of these apparatuses are Tattersall two-points workability device, BML viscometer, IBB rheometer, BTRheom, and Slump rate machine (SLRM-II). Tattersall two-point workability device is one of the earliest methods developed to measure the rheology of fresh concrete by measuring the torque required to turn an impeller in concrete. The device consists of a stationary bowl mounted in a large frame and a hydraulic motor used to turn the impeller immersed in the concrete sample. The device also has a vibrator to measure the behaviour of fresh concrete under the effects of vibration. The concrete in this test is assumed to obey Bingham model. The device has been used widely in research, but its large size limits its use in the field (ACI 238, 2008). The BML viscometer is a coaxial cylinder rheometer which consists of outer rotating cylinder and internal vertical blades. During the test, the torque acting on the blades is measured while the outer cylinder is rotating. The viscometer is intended for concrete with slump more than 120 mm (ACI 238, 2008). The IBB rheometer is a modification of Tattersall two-point workability device which was developed to measure the rheology of wet-mix shotcrete. The rheometer consists of a rotating impeller and a fixed cylindrical container. During the test, a load cell measures the reaction torque from the impeller and a tachometer measures the speed of the impeller. A portable version of the IBB rheometer has been developed. One of the advantages of this rheometer that it can be used for a wide range of concrete workability (ACI 238, 2008). BTRheom is a parallel plate rheometer that is used to measure the rheological properties of fresh concrete. It consists of two parts, the fixed part and rotating part. The BTRheom determines the flow properties by turning the rotating part with different speeds and measuring the resultant torque at these speeds. All operations of the BTRheom are computer controlled. Moreover, it allows for measurements under vibration (ACI 238,

2008). ACI 238 (2008) provides a comprehensive list and assessment of workability test methods.

The slump rate machine, SLRM-II, is a modified slump test which has introduced the variable of time to the standard test. The time variable is used to measure plastic viscosity, while yield stress is measured from the slump flow value. Hence, two points are provided to characterize the fresh concrete flow (Chidiac et al., 2003). The SLRM-II apparatus consists of two parts; the cone lifter part and the predicting part as shown in Figure 2.4. The first part is provided with hydraulic oil system to lift the slump cone with a constant rate. The second part consists of ten sensors to monitor the withdrawal rate of the cone and slump of the concrete. Such monitoring is used to measure the concrete slump, time of slump, and slumping rate, while the slump flow is measured manually. Subsequently, these values are substituted in a mathematical models for estimating the yield stress and the plastic viscosity of the concrete. Additional information on this apparatus can be found in Chidiac and Habibbeigi (2005).

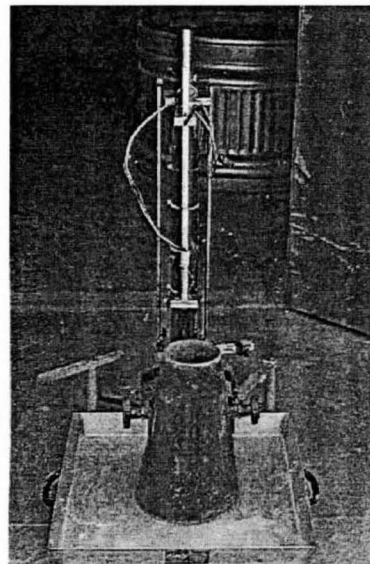


Figure 2.4: Slump rate machine (SLRM-II)

Many models have been developed to relate the yield stress and plastic viscosity to the slump value and slump time, respectively. Tanigawa et al. (1992) used the principle of applied mechanics to establish a relationship between the yield stress and slump value (Tanigawa et al., 1992). They assumed that the stress is developed due to the weight of fresh concrete only and neglected the stresses in the other direction. They proposed the following equation

$$\tau_y = \frac{\alpha \rho g (H - S_1)}{\sqrt{3}} \quad (2.5)$$

where  $\tau_y$ (Pa) is the yield stress,  $S_1$ (m) the slump,  $\rho$ ( $kg/m^3$ ) the fresh concrete density,  $\alpha$  the shape factor, and  $g$ ( $m/s^2$ ) is the gravitational constant.

Chidiac et al. (2000) provided an improvement to Tanigawa et al. (1992) model by eliminating the shape factor. They related the yield stress to the slump flow instead of slump value (Chidiac et al., 2000) where

$$\tau_y = \frac{4gV\rho}{\sqrt{3}\pi S_f^2} = 0.0397 \left( \frac{\rho}{S_f^2} \right) \quad (2.6)$$

In 2006, Chidiac et al., (2006) proposed an empirical model which relates the yield stress to the slump value and slump flow. This model, which combines the work of Hu et al. (1996) and Chidiac et al. (2000), is given by

$$\tau_y = \rho \left( 1.85 (0.3 - S_1) + \left( \frac{0.0198}{S_f} \right) \right) \quad (2.7)$$

Regarding the plastic viscosity, Chidiac et al. (2000) have followed the work of Tanigawa et al. (1992) and developed a model which relates the slump value to the plastic viscosity, slumping time, concrete density and shape factor

$$S_1 = H - \frac{1}{\frac{\alpha \rho g}{600\eta} t + \frac{1}{H}} \quad (2.8)$$

where  $\eta$ (Pa.s) is the plastic viscosity,  $t$ (s) the slump time, and  $H$  (m) is the height of the slump cone. By substituting the slump flow, and final time of slump, they

rewrote Equation 2.8 so viscosity can be calculated from the slump, slump flow, final time of slump and concrete density, i.e.

$$\eta = \frac{\rho g H V}{150 \pi S_1 S_f^2 t_{slump}} \quad (2.9)$$

## 2.5 Using Rheology in Concrete Mixture Proportioning

Concrete mixture is proportioned to achieve specific design characteristics such as strength and durability as well as transporting, placing and finishing. This process is complicated. For example, a high strength concrete which requires a low water-cement ratio, yields a low slump value. Having a stiff mix creates problems with placement and compaction. One remedy is to add a high dosage of water reducing agent, this will result in an increase in the slump. However, a high slump concrete enhances the placeability and pumpability, but it can create problems with the finishing and stability. Therefore, the target properties have to be adequately balanced. This is one of many reasons why rheological properties need to be included in the design of concrete mixtures. Two additional cases studied are presented to reflect the importance of rheological properties in the design and control of concrete mixtures.

### 2.5.1 Pumpability

Pumping which is an efficient way to transport and place concrete, is strongly influenced by the concrete plastic viscosity (De larrad et al., 1997). It has been shown that increasing the plastic viscosity will result an increase in the pumping resistance. On the other side, the yield stress has a little effect on pumpability. Figure 2.5 shows the relationship between the plastic viscosity and the pumping resistance. In this relationship, the pumping resistance is represented by the ratio between the pumping



pressure and number of strokes per minute (De larrad et al., 1997).

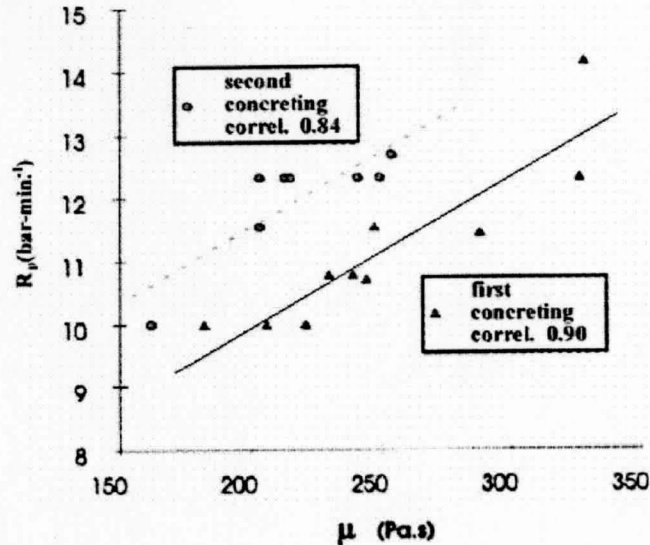


Figure 2.5: Plastic viscosity and pumping resistance relationship (F. de larrad, 1999)

### 2.5.2 Consistency and stability

Consistency is a term used to qualitatively describe the flow of fresh concrete. However, consistency can be quantitatively characterized by the yield stress (F. de larrad, 1999). Concrete that has a sticky consistency tends to have problems with the finishing. On the other side, a flowable concrete can create problems with stability. Hence, the consistency of fresh concrete has to be chosen to balance between the placing requirements and finishing conditions. In this essence, the yield stress can be used to control the consistency of fresh concrete. To illustrate this point, one can examine a 200 mm thick slab that needs to be cast with 6 percent slope. Using the free body diagram of Figure 2.6, one can calculate the minimum yield stress on the basis of equilibrium, i.e.,

$$\tau_o = \rho g h \sin\theta \quad (2.10)$$

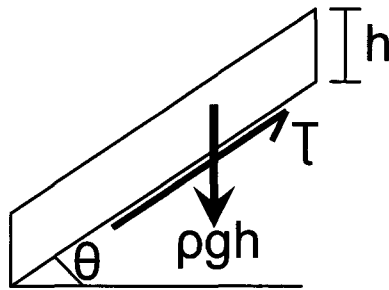


Figure 2.6: Equilibrium of fresh concrete under gravity (F. de larrad, 1999)

On the other side, the maximum value of yield stress is dictated by the construction type and placing condition. The maximum yield stress is limited by the flowability of the concrete (F. de larrad, 1999).

## Chapter 3

# Experimental Program

The factorial design is “a type of experimental design in which every level of one factor is tested in combination with every level of another factor. In general, in a factorial experiment, all possible combinations of factor levels are tested” (Montgomery and Runger, 2003). In this research, the factorial design was adopted to study the influence of concrete mixture proportions on concrete fresh and hardened properties. Such a study enables one to establish proportionality between concrete mixture and slump, yield stress, plastic viscosity and 28-day compressive strength. To meet the objective of this study, six variables, namely water-cement ratio, water content, maximum coarse aggregate size, percent addition of silica fume, percent addition of slag and bulk volume of coarse aggregate, were identified. The range for each mix design variable was chosen to meet the definition of normal concrete as stipulated in Design and Control of Concrete Mixture (CAC, 2002).

This chapter consists of four sections. First section presents the concrete mixtures studied and the methodology adopted for choosing the range for the selected mix design variables. This is followed by the fractional factorial design method employed to design the concrete mixtures for this experimental program. Characterization of the materials used in the experimental program is carried out in Section three. Finally,

Section four presents the experimental procedure and test method used to evaluate the properties of fresh concrete and compressive strength of hardened concrete.

### 3.1 Concrete Mix Design

Recognizing that workability of concrete depends on the concrete mixture, the influence of six mix-design variables on the properties of fresh concrete was studied. The six variables are water-cement ratio (w/c), water content, maximum aggregate size, percent addition of silica fume, percent addition of slag and the bulk volume of coarse aggregate. Following the statistical factorial design method, two levels, low and high values, for each variable are required (Montgomery and Runger, 2003). The levels were chosen according to the concrete mixture proportioning method of Cement Association of Canada (CAC, 2002). The design target was an air entrained normal concrete with a compressive strength greater than 20 MPa and a slump value greater than 75 mm. According to Table 2.1, this corresponds to a w/c value of 0.6. A minimum value of 0.4 was chosen for w/c to maintain economical mixes. Regarding the maximum coarse aggregate size, the two levels were chosen to correspond to the commonly used sizes, namely 14 and 20 mm. The low and high levels of water content were chosen, respectively, as 193 and 205 kg/m<sup>3</sup> for the 14 mm coarse aggregate, and 184 and 197 kg/m<sup>3</sup> for the 20 mm coarse aggregate. According to Table 2.2, these values are expected to yield 75 mm and 175 mm slump for an air entrained concrete. The levels of percent replacement of silica fume and slag were chosen within the recommended range of ACI 318 (ACI 318, 2005). These levels are 0 to 30% for slag and 0 to 8% for silica fume, as a replacement ratio of cement content. Lastly, the two levels of the bulk volume of coarse aggregate per unit volume of concrete were chosen as per the recommended values given in Table 2.3. For fine aggregate with a fineness modulus of 2.72, the recommended bulk volume of dry rodded coarse aggregate per

unit volume of concrete is 0.56 for the 14 mm aggregate and 0.63 for the 20 mm aggregate. For this study, the two levels of coarse aggregate volume were chosen as plus and minus 10% of the recommended values. This led to the levels of 0.5 and 0.62 for the 14 mm aggregate and 0.57 and 0.69 for the 20 mm aggregate.

### 3.2 Fractional Factorial Design

Fractional factorial design of resolution six ( $2^{6-1}$ ) was adopted to study the effect of one variable and the interaction effects of two variables. According to this model, a set of 32 mixes are required. These mixes vary between -1 and +1 coded values for each variable. The codes and values attributed to the variables are given in Table 3.1. The coded values are computed according to Montgomery and Runger (2003) where

$$\text{Coded Value} = \frac{\text{Value} - \text{Mean}}{\text{Range}/2} \quad (3.1)$$

Table 3.1: Variables and corresponding coded values adopted for the experimental program

Coded Value		-1	0	+1
Variables				
w/c		0.4	0.5	0.6
Water content (kg/m <sup>3</sup> )	14 mm	193	199	205
	20 mm	184	190.5	197
Coarse aggregate size (mm)		14	-	20
Silica fume (%)		0	-	8
Slag (%)		0	-	30
Coarse aggregate content	14 mm	0.5	0.56	0.62
	20 mm	0.57	.63	0.69

Since the effect of the mix variables on the relevant responses could vary in a nonlinear manner, a set of star points, with different levels of variables, was added. Such points enable one to assess the influence of the variable in four levels instead of just two levels. In this context, 4 mixes with different levels of w/c, water content and coarse aggregate content were added. The w/c levels were 0.5 and 0.7, the water content 175 and 205 kg/m<sup>3</sup>, and the bulk volume of coarse aggregate 0.5 and 0.62. The other variables were assumed constant, i.e., 14 mm for maximum aggregate size and 0% replacement ratio for silica fume and slag. In addition, 3 mixes with different levels of replacement ratio of slag were added. These levels were 0, 20 and 40%, while the other variables were kept constant, i.e., 0.5 for w/c, 199 kg/m<sup>3</sup> for water content, 14 mm for maximum aggregate size, 0% replacement ratio for silica fume and 0.56 for bulk volume of coarse aggregate. Also, two mixes with different levels of coarse aggregate content were added. Such levels have been chosen in the same way as in designing the main points but multiplied by plus and minus 20% instead of 10%. These levels were 0.448 and 0.672 for the bulk volume of coarse aggregate, while the other variables were kept constant, i.e., 0.5 for w/c, 199 kg/m<sup>3</sup> for water content, 14 mm for maximum aggregate size and 0% replacement ratio for silica fume and slag. In summary, 41 mixes were developed for this experiment to include the fractional factorial design main points and star points. Air entraining agent was added using a constant dosage of 35 ml per 45 kg/m<sup>3</sup> of cement content, for all the mixes. Hence, the developed model is expected to be air entrained, normal concrete with w/c range of 0.4 to 0.7, water content of 175 to 205 kg/m<sup>3</sup>, maximum aggregate size of 14 to 20 mm, replacement ratio of silica fume of 0 to 8% and slag of 0 to 40%, and bulk volume of coarse aggregate of 0.45 to 0.69. In addition, four concrete mixtures with random proportions were added to validate the model. The corresponding 45 concrete mixtures designed for this experimental program are given in Tables 3.2 and 3.3.

Table 3.2: Design of concrete mixtures adopted for this study -Main points

Mix	Mix label	w/c	Water (kg/m <sup>3</sup> )	Size (mm)	Silica fume (%)	Slag (%)	Coarse aggregate (Bulk volume)
1	44	0.4	193	14	0	0	0.50
2	42	0.6	193	14	0	0	0.62
3	38	0.4	205	14	0	0	0.62
4	43	0.6	205	14	0	0	0.50
5	40	0.4	184	20	0	0	0.69
6	45	0.6	184	20	0	0	0.57
7	39	0.4	197	20	0	0	0.57
8	41	0.6	197	20	0	0	0.69
9	19	0.4	193	14	8	0	0.62
10	14	0.6	193	14	8	0	0.50
11	20	0.4	205	14	8	0	0.50
12	15	0.6	205	14	8	0	0.62
13	18	0.4	184	20	8	0	0.57
14	16	0.6	184	20	8	0	0.69
15	21	0.4	197	20	8	0	0.69
16	17	0.6	197	20	8	0	0.57
17	23	0.4	193	14	0	30	0.62
18	22	0.6	193	14	0	30	0.50
19	26	0.4	205	14	0	30	0.50
20	24	0.6	205	14	0	30	0.62
21	27	0.4	184	20	0	30	0.57
22	25	0.6	184	20	0	30	0.69
23	28	0.4	197	20	0	30	0.69
24	29	0.6	197	20	0	30	0.57
25	35	0.4	193	14	5.6	30	0.50
26	31	0.6	193	14	5.6	30	0.62
27	32	0.4	205	14	5.6	30	0.62
28	34	0.6	205	14	5.6	30	0.50
29	30	0.4	184	20	5.6	30	0.69
30	37	0.6	184	20	5.6	30	0.57
31	33	0.4	197	20	5.6	30	0.57
32	36	0.6	197	20	5.6	30	0.69

Table 3.3: Design of concrete mixtures adopted for this study -Star points

Mix	Mix label	w/c	Water (Kg/m <sup>3</sup> )	Size (mm)	Silica Fume (%)	Slag (%)	Coarse aggregate (Bulk volume)
33	55	0.5	193	14	0	0	0.50
34	52	0.7	175	14	0	0	0.50
35	54	0.5	205	14	0	0	0.50
36	57	0.7	193	14	0	0	0.50
37	51	0.5	193	14	0	0	0.62
38	60	0.7	175	14	0	0	0.62
39	49	0.5	205	14	0	0	0.62
40	58	0.7	193	14	0	0	0.62
41	47	0.5	199	14	0	20	0.56
42	48	0.5	199	14	0	40	0.56
43	62	0.5	199	14	0	0	0.45
44	63	0.5	199	14	0	0	0.67
45	46	0.5	199	14	0	0	0.56

### 3.3 Material

Concrete was prepared using mixtures of crushed limestone, siliceous sand, ordinary Portland cement, ordinary Portland cement blended with silica fume, ground granulated blast-furnace slag, air entraining agent and water.

#### 3.3.1 Aggregates

Crushed limestone aggregate, which was obtained from Lafarge North America's Dundas quarry located in Dundas, Ontario, with a maximum size of 14 and 20 mm, was used in this study. The particles gradation curves corresponding to the 14 mm and 20 mm coarse aggregate, obtained in accordance with CSA test method A23.2-2A (CSA, 2000), are shown in Figure 3.1 and Figure 3.2, respectively. The results show that the aggregates are well graded and within the CSA standard limits. The specific gravity of the 14 mm and 20 mm coarse aggregate, which were measured according



to CSA test method A23.2-12A (CSA, 2000), are 2.74 and 2.75, respectively. The saturated surface dry moisture contents, which were measured according to the CSA test method A23.2-12A, are 0.88% and 0.92%, respectively for the 14 mm and 20 mm coarse aggregate. The oven dry bulk densities, measured according to CSA test method A23.2-10A (CSA, 2000), are 1576 kg/m<sup>3</sup> for the 14 mm and 1636 kg/m<sup>3</sup> for the 20 mm coarse aggregate.

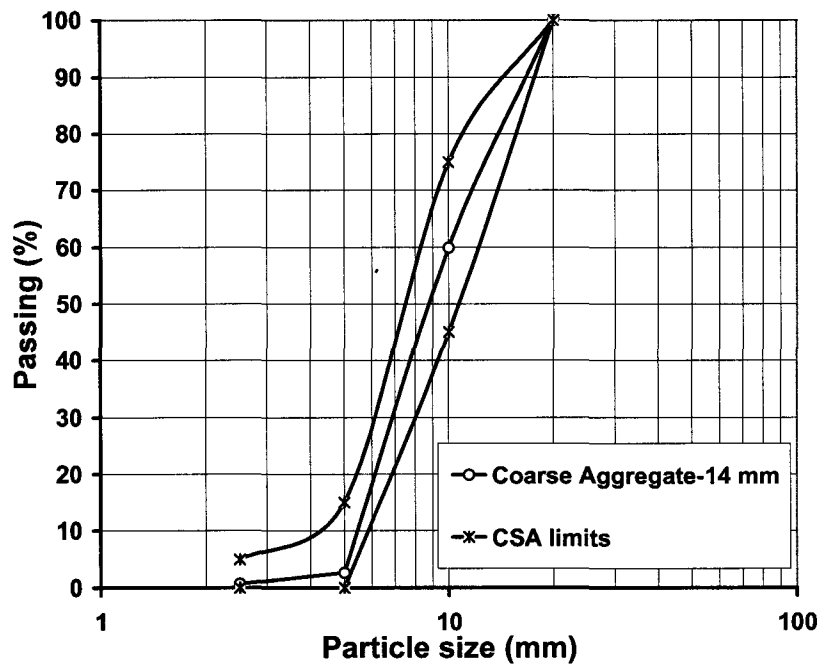


Figure 3.1: 14 mm coarse aggregate particle size distribution curve

Silicious sand obtained from Lafarge North America's west Paris plant, which was used as fine aggregate for all the mixes, possesses a fineness modulus of 2.72. Following the procedure of CSA test method A23.2-6A (CSA, 2000), the specific gravity of sand is found equal to 2.71, the saturated surface dry moisture content equal to 1.58% and the dry packing density equal to 1812 kg/m<sup>3</sup>. The sand particle size distribution is shown in Figure 3.3. The results indicate that the particles distribution are within the limits of CSA test method A23.2-2A (CSA, 2000).

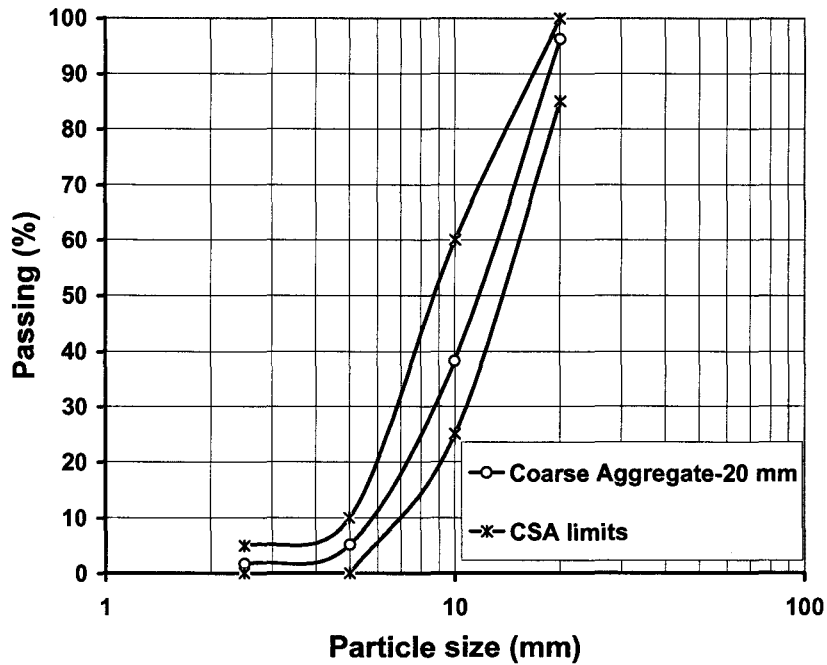


Figure 3.2: 20 mm coarse aggregate particle size distribution curve

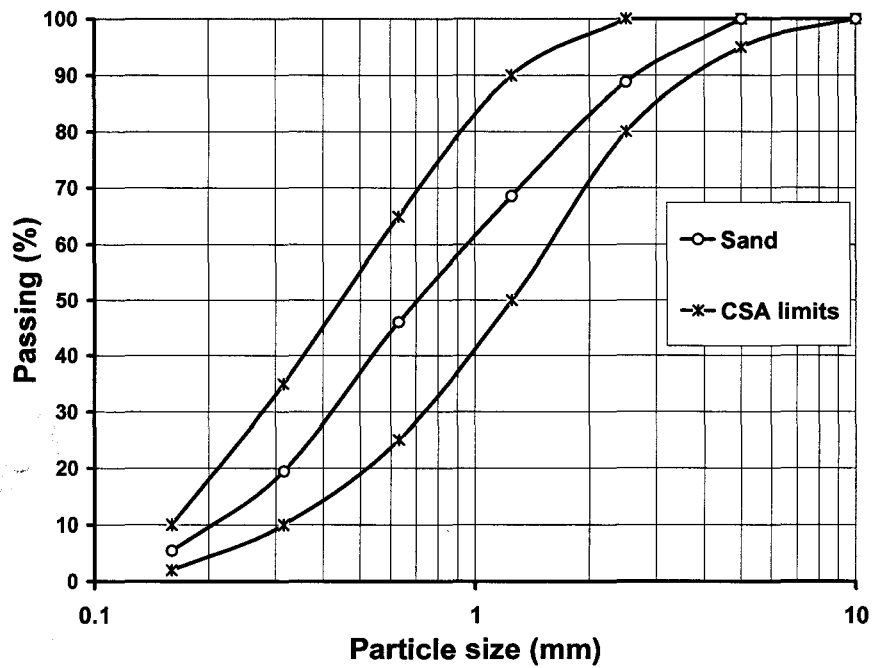


Figure 3.3: Fine aggregate particle size distribution curve

### 3.3.2 Cementitious material

Three cementitious materials were used in this study; ordinary Portland cement (Hydraulic Cement type GU-type 10), ordinary Portland cement blended with 8% silica fume (GUb-SF Cement type IP 8), and ground granulated blast-furnace slag (GG-BFS) grade 80. The material was obtained from Lafarge North America. The corresponding chemical and physical properties are given in Table 3.4 and Table 3.5.

### 3.3.3 Air entraining agent

Air entraining agent, which is Micro Air and manufactured by BASF Construction Chemicals (Master Builders), was used in this study. The admixture meets the requirements of ASTM C260 (BASF, 2007). Dosage of 35 ml per 45 kg/m<sup>3</sup> of cement content was used according to the manufacturer's recommended dosage.

## 3.4 Experimental Procedure

The same experimental procedure was adopted for all the mixes. This includes mixing procedure, and test methods to evaluate the properties of fresh concrete and hardened concrete. The general procedure followed for this experimental program is as follows:

1. Prepare the ingredients according to the mix design.
2. Mix the ingredients according to the mixing procedure.
3. Test the properties of fresh concrete, namely the slump, slump flow, slump rate, density, air content, yield stress and plastic viscosity.
4. Prepare three cylinders to test the 28-day compressive strength.
5. Test the compressive strength of the concrete after 28 days.

Table 3.4: Chemical and physical properties of Hydraulic Cement GU-type 10 and GUb-SF Cement type IP 8

	<b>Hydraulic Cement GU-type 10</b>	<b>GUb-SF Cement type IP 8</b>
SiO <sub>2</sub> (%)	19.7	25.4
Al <sub>2</sub> O <sub>3</sub> (%)	4.9	5.1
Fe <sub>2</sub> O <sub>3</sub> (%)	2.4	2.6
CaO (%)	62.2	57.6
MgO (%)	3.1	2.7
SO <sub>3</sub> (%)	3.4	2.6
FCaO (%)	1.3	1.7
Loss on Ignition (%)	2.9	2.5
Equivalent Alkalies (%)	0.75	0.76
Silica Fume Addition (%)	-	8
Specific Surface Area (Blaine)	4280	5890
% Passing 325 (45um) Mesh (%)	90.7	88.8
Time of Setting-Initial (min)	115	110
Compressive Strength - 3 Day (MPa)	27.6	23.7
Compressive Strength - 7 Day (MPa)	34.4	33.6

Table 3.5: Chemical and physical properties of Ground granulated blast-furnace slag (GGBFS)

	<b>GGBFS</b>
SiO <sub>2</sub> (%)	34.5
Al <sub>2</sub> O <sub>3</sub> (%)	9.9
Fe <sub>2</sub> O <sub>3</sub> (%)	0.7
CaO (%)	36.5
MgO (%)	12.3
SO <sub>3</sub> (%)	3.5
K <sub>2</sub> O (%)	0.4
Na <sub>2</sub> O (%)	0.3
TiO <sub>2</sub> (%)	0.7
Mn <sub>2</sub> O <sub>3</sub> (%)	0.7
Naeq (%)	0.6
Retained on 45 micron (%)	2
Specific gravity	2.92
Compressive Strength - 7 Day (MPa)	22

Additional details for the above noted procedures are given next.

### 3.4.1 Mixing procedure

Concrete was mixed in a pan mixer and according to the following procedure 1) Add the air entraining agent to the water and mix for 30 seconds; 2) Add the coarse aggregate, fine aggregate, cement and 1/3 of the water content to the mixer; 3) Mix for 2 minutes; 4) Add the remaining water while the mixer is running; 5) Continue mixing for 2 minutes; 6) Stop the mixer for 1 minute; 7) Mix for 1 minute.

### 3.4.2 Slump and slump flow

The slump was measured according to CSA test method A23.2-5C (CSA, 2000). This test was carried out after dumping the concrete from the mixer. The slump flow, which is a measure of the concrete spread in two-perpendicular directions, was also measured from the slump test. Figure 3.4 shows the slump of Mix label #41.

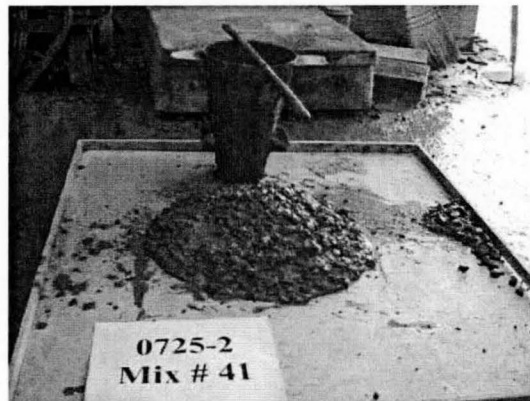


Figure 3.4: Slump test of Mix label #41

### 3.4.3 Density and air content

The density of fresh concrete and air content were measured for each mix according to CSA test method A23.2-4C (CSA, 2000). Figure 3.5 shows the pressure vessel used to measure the concrete's air content. The same container was also used to evaluate the density of fresh concrete.

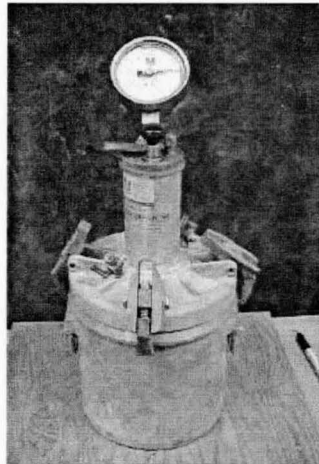


Figure 3.5: Pressure vessel used to measure air content

### 3.4.4 Yield stress and plastic viscosity

The slump rate machine (SLRM-II), shown in Figure 3.6, was used to measure the slump, slump flow, slump time and slump rate of the concrete (Chidiac and Habibbeigi, 2005). This test method permits the calculations of yield stress and plastic viscosity by assuming that the concrete flow obeys Bingham model.

### 3.4.5 Compressive strength test

For each concrete mix, 3 cylinders, 100 mm by 200 mm, were cast for testing of 28-day compressive strength of concrete. Concrete was moist cured for 28 days. The

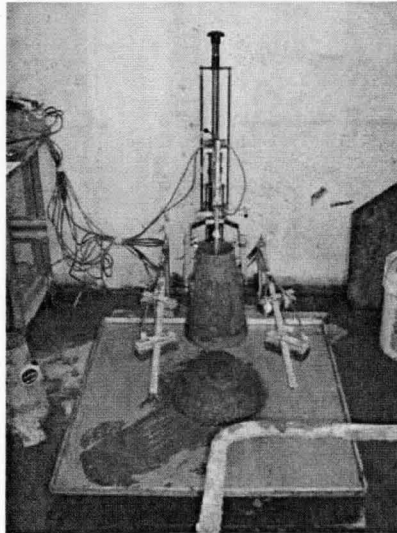


Figure 3.6: Slump Rate Machine (SLRM-II)

compressive strength was measured according to CSA test method A23.2-9C (CSA, 2000). Figure 3.7 shows the apparatus used to conduct this test.



Figure 3.7: Tinius Olsen Universal testing machine 600-KN used to test the concrete 28-day compressive strength



# Chapter 4

## Experimental Results and Analyses

In this chapter, the results of the experimental program described in Chapter 3 are presented. A comparison between the design values and measured values is carried out in addition to the statistical analysis of the results to determine the effects of mix design variables on the rheological properties of fresh concrete and compressive strength. Mathematical models based on the statistical factorial design were derived to examine the influence of concrete mixture and their interaction on concrete fresh and hardened properties. Regression models were derived for slump, slump flow, yield stress, plastic viscosity and 28-day compressive strength. Linear and nonlinear functions were evaluated for modeling the effect of each variable on the relevant responses. Moreover, the statistical significance of the variables was evaluated.

### 4.1 Results

Measured values, namely slump, slump flow, entrained air content, density and compressive strength are shown in Tables 4.1 and 4.2. In addition, the results obtained using the SLRM-II, namely slump, slump flow, time of slump are given in Tables 4.3 and 4.4.

Table 4.1: Slump, slump flow, density, air content and 28-day compressive strength of concrete mixtures -Main points

Mix	Mix label	Slump (mm)	Slump flow (mm)	Density (kg/m <sup>3</sup> )		Entrained air (%)		28-day Compressive strength (MPa)		
1	44	100	228	2298	2299	5.8	5.9	35	40	39
2	42	190	320	2292	2292	5.2	5.3	22	24	16
3	38	120	233	2315	2313	4.8	4.9	37	37	35
4	43	220	430	2284	2285	5.1	5.1	28	26	23
5	40	80	200	2361	2356	4.5	4.7	37	34	36
6	45	190	320	2284	2291	5.6	5.6	22	26	25
7	39	95	228	2342	2336	4.8	4.9	37	40	39
8	41	215	430	2353	2361	3.0	3.2	21	25	25
9	19	55	213	2308	2313	5.4	5.3	43	42	39
10	14	180	350	2257	2221	7.5	7.5	28	28	27
11	20	95	228	2275	2278	5.8	5.7	46	39	43
12	15	210	350	2281	2274	5.9	5.8	28	28	28
13	18	65	223	2320	2336	5.5	5.5	41	42	38
14	16	170	290	2319	2333	5.0	5.0	28	28	29
15	21	95	203	2299	2303	5.6	5.5	34	35	36
16	17	215	385	2284	2288	5.0	5.1	29	30	30
17	23	110	218	2343	2340	4.7	4.7	42	40	42
18	22	200	375	2248	2252	6.6	7.0	24	25	23
19	26	135	263	2293	2292	5.3	5.2	37	39	34
20	24	225	395	2326	2322	4.1	4.2	29	27	26
21	27	100	215	2333	2333	5.0	5.2	37	38	37
22	25	180	370	2339	2342	4.1	4.0	27	25	26
23	28	100	218	2325	2337	4.4	4.2	36	38	34
24	29	210	385	2332	2335	4.1	4.0	25	27	26
25	35	95	220	2281	2293	5.5	5.3	42	39	41
26	31	190	305	2281	2291	5.1	5.1	30	28	30
27	32	100	205	2289	2308	4.7	4.6	42	39	42
28	34	220	430	2252	2274	5.3	5.3	29	31	31
29	30	85	208	2306	2313	5.3	5.3	37	36	36
30	37	195	315	2282	2275	5.2	5.2	29	27	29
31	33	90	215	2320	2326	4.3	4.4	39	41	41
32	36	200	438	2320	2329	3.7	3.8	28	29	25

Table 4.2: Slump, slump flow, density, air content and 28-day compressive strength of concrete mixtures -Star points

Mix	Mix label	Slump (mm)	Slump flow (mm)	Density (kg/m <sup>3</sup> )		Entrained air (%)		28-day Compressive strength (MPa)		
33	55	200	365	2276	2279	5.6	5.7	30	30	31
34	52	140	248	2192	2189	8.7	8.9	14	16	15
35	54	227	435	2276	2279	5.0	5.1	33	32	34
36	57	210	375	2223	2220	7.5	7.5	18	18	19
37	51	195	300	2284	2305	5.1	5.1	28	33	31
38	60	175	293	2200	2207	8.5	8.8	14	13	14
39	49	195	305	2293	2303	4.8	4.7	32	33	27
40	58	210	395	2276	2291	5.5	5.7	17	20	15
41	47	190	338	2296	2303	5.0	5.0	32	33	34
42	48	190	305	2295	2306	4.8	4.6	34	30	31
43	62	185	360	2211	2211	7.7	7.8	26	26	27
44	63	190	360	2261	2254	6.6	6.7	26	27	24
45	46	175	328	2307	2301	5.0	5.0	32	31	33

Table 4.3: Slump, slump flow, slump time, yield stress and plastic viscosity of concrete mixtures obtained using SLRM-II -Main points

Mix	Mix label	SLRM-II					
		Slump (mm)	Slump Flow (mm)	Slump time (s)	Yield Stress (Pa)	Plastic Viscosity (Pa.s)	
						Proposed Model	Chidiac Model
1	44	97	228	3.12	1761	38	49
2	42	199	295	2.73	1045	18	12
3	38	116	245	2.73	1529	27	31
4	43	214	375	2.32	644	7	6
5	40	75	205	3.11	2226	50	80
6	45	185	320	2.73	886	13	11
7	39	101	210	3.11	2103	46	56
8	41	200	395	3.50	599	18	9
9	19	50	205	1.95	2181	50	73
10	14	218	345	2.34	746	15	7
11	20	91	230	2.34	1707	30	38
12	15	244	368	2.33	669	13	6
13	18	52	210	1.95	2094	50	68
14	16	173	363	3.11	702	16	11
15	21	94	210	3.10	2070	45	59
16	17	251	390	2.71	596	11	6
17	23	83	223	2.33	1876	35	46
18	22	187	315	1.95	899	10	8
19	26	128	270	2.72	1247	19	23
20	24	198	410	2.33	548	11	6
21	27	86	200	2.73	2313	50	64
22	25	178	380	2.72	643	14	9
23	28	121	215	3.10	2000	40	44
24	29	209	408	2.34	557	13	5
25	35	83	205	3.11	2159	50	70
26	31	191	310	2.72	943	20	12
27	32	91	218	3.12	1927	42	57
28	34	226	363	1.56	683	11	4
29	30	97	200	2.71	2290	47	55
30	37	213	340	2.72	782	18	9
31	33	87	208	2.72	2140	40	58
32	36	216	448	2.72	460	15	5

Table 4.4: Slump, slump flow, slump time, yield stress and plastic viscosity of concrete mixtures obtained using SLRM-II -Star points

Mix	Mix label	SLRM-II					
		Slump (mm)	Slump Flow (mm)	Slump time (s)	Yield Stress (Pa)	Plastic Viscosity (Pa.s)	
						Proposed Model	Chidiac Model
32	36	216	448	2.72	460	15	5
33	55	183	350	1.55	738	10	5
34	52	142	250	2.73	1390	23	23
35	54	249	400	2.33	565	8	5
36	57	194	350	2.34	719	10	8
37	51	195	323	2.34	875	15	9
38	60	180	323	2.34	840	17	9
39	49	201	325	2.71	863	15	10
40	58	174	388	2.73	603	13	8
41	47	190	340	3.11	789	10	11
42	48	188	340	2.73	789	13	10
43	62	180	340	1.93	759	9	7
44	63	196	348	2.73	741	15	9
45	46	193	315	2.34	921	15	10

Two models were employed to predict the rheological properties. The first one is based on the work of Chidiac et al. (2000), where the plastic viscosity is determined based on the slump, slump flow, density and time of slump according to the following equation:

$$\eta = \frac{\rho g H V}{150 \pi S_l S_f^2 t_{slump}} \dots \dots \dots (2.9)$$

The second method, which is the proposed method, can be considered a refinement to the previous work. It assumes that at the onset of slump, the flow of concrete is impeded by the slump cone (Chidiac and Habibbeigi, 2005) and a true measurement is difficult to obtain. Moreover, the proposed method assumes that as the concrete reaches its final slump, the shear stress and strain rate are much lower in comparison to the state when the concrete starts to slump and therefore contain errors and need to be discarded. Accordingly, the proposed method employees the same fundamentals as the one reported by Chidiac et al. (2000) but ignores the first two slump versus time measurements and the last two measurements. The relation reported by Chidiac et al. (2000), which relates slump to time, density, and plastic viscosity, was used for the proposed method, namely

$$S_l = H - \frac{1}{\frac{\alpha \rho g}{600 \eta} t + \frac{1}{H}} \dots \dots \dots (2.8)$$

The least square approach was used to fit the curve to the experimental measurements. The unknown variable is plastic viscosity. To illustrate the difference between the two rheological models, the experimental slump-time curves corresponding to Mixes label #38, 52, 25 and 29 are shown respectively in Figures 4.1 to 4.4. Results of Figures 4.1 and 4.2 show that the viscosity measured by the two models are similar when the flow of concrete is consistent, and they are different as shown in Figures 4.3 and 4.4 when the flow is disturbed as the ones for Mixes label #25 and 29. Accordingly, the proposed method is expected to yield more consistent predictions of the plastic viscosity.

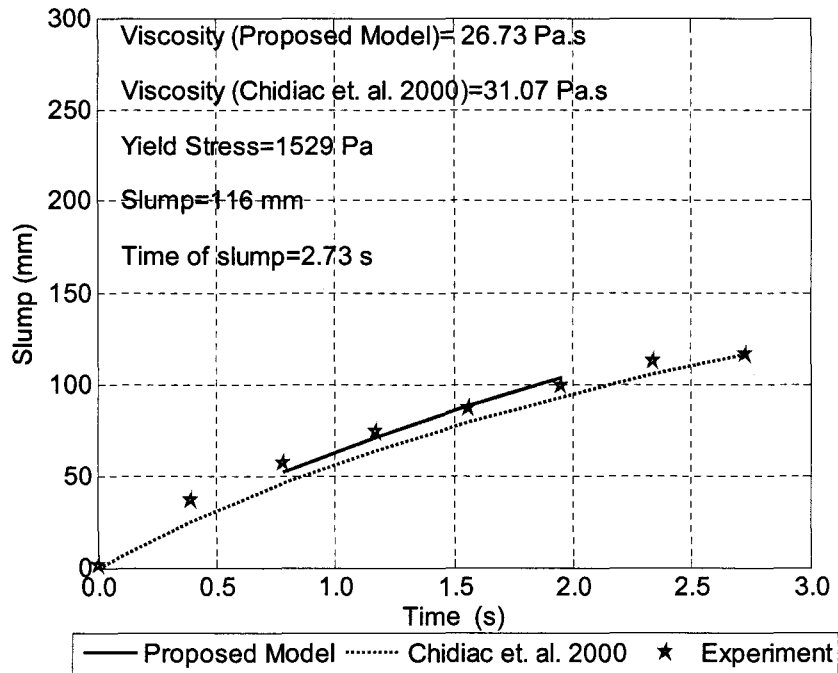


Figure 4.1: Slump-time curve for Mix label #38

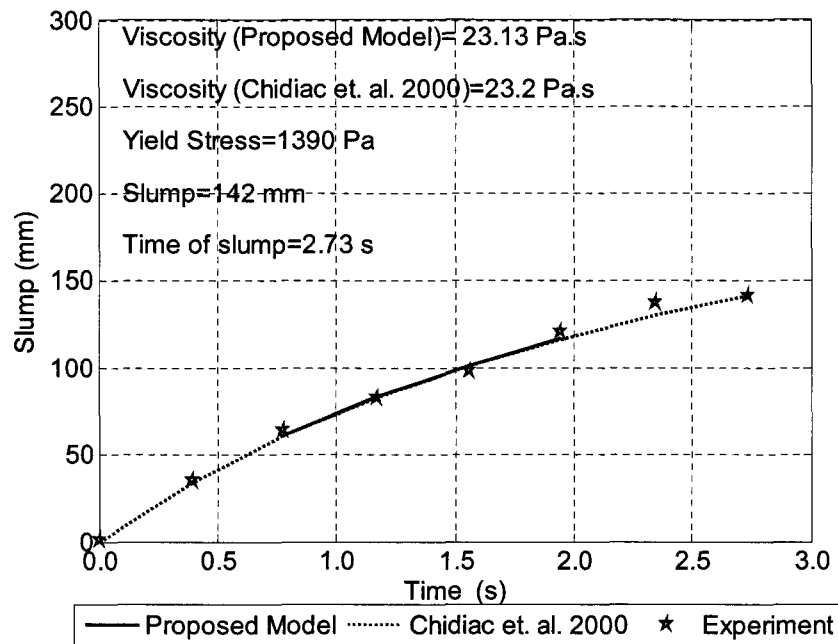


Figure 4.2: Slump-time curve for Mix label #52

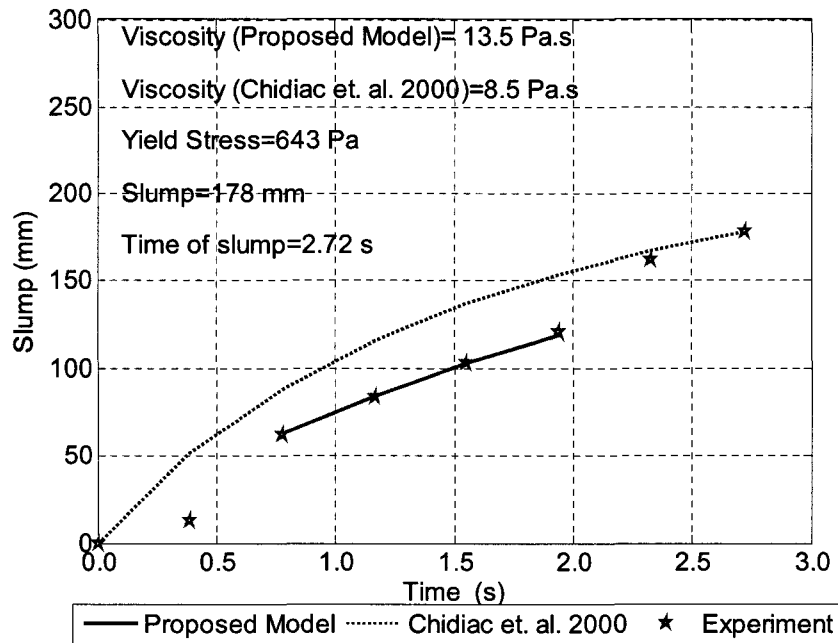


Figure 4.3: Slump-time curve for Mix label #25

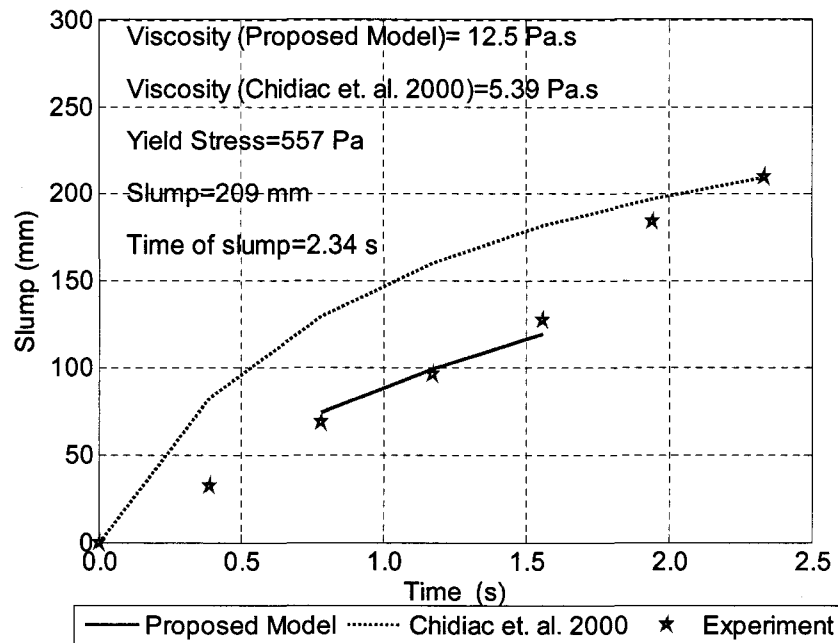


Figure 4.4: Slump-time curve for Mix label #29



The yield stress is calculated according to Chidiac et al. (2000) using the following relation:

$$\tau_y = \frac{4gV\rho}{\sqrt{3}\pi S_f^2} = 0.0397 \left( \frac{\rho}{S_f^2} \right) \dots\dots\dots(2.6)$$

Computed rheological properties, yield stress and plastic viscosity are given in Tables 4.3 and 4.4.

## 4.2 Analysis of Experimental Data

Measured values of slump and compressive strength are first compared with the design values. This comparison will provide an assessment of the adequacy of the CAC guidelines to design and control concrete mixtures.

### 4.2.1 Slump

The slump was measured using the traditional slump test and the automated slump rate machine. The measured slump values were also compared to the design values defined in accordance with design guidelines of CAC (2002). These results are given in Tables 4.5 and 4.6. Evaluation of the results shows that the measured slump is found to be within the design value for 5 out of 45 mixes for the traditional test, and 5 or 6 out of 45 mixes for the SLRM-II. This implies that 13% of the concrete mixtures have representative workability measurements. These results indicate that the slump as a design and control parameter is a very poor metric, and that CAC guidelines are not adequate in this regard.

### 4.2.2 Slump Flow

Slump flow, which is a measure of the concrete spread, has been proposed as the metric for high slump concrete such as self consolidating concrete. Although normal slump

Table 4.5: Measured slump according to CAC guidelines versus the measured slump using the traditional slump test and SLRM-II -Main points

Mix	Mix label	Slump (mm)			Difference (%)		
		CAC	Traditional test	SLRM-II	Slump test vs. CAC	SLRM-11 vs. CAC	Slump test vs. SLRM-11
1	44	75 - 100	100	97	14	11	3
2	42	75 - 100	190	199	117	127	-5
3	38	150 - 175	120	116	-26	-29	3
4	43	150 - 175	220	214	35	32	3
5	40	75 - 100	80	75	-9	-14	7
6	45	75 - 100	190	185	117	111	3
7	39	150 - 175	95	101	-42	-38	-6
8	41	150 - 175	215	200	32	23	8
9	19	75 - 100	55	50	-37	-43	10
10	14	75 - 100	180	218	106	149	-17
11	20	150 - 175	95	91	-42	-44	4
12	15	150 - 175	210	244	29	50	-14
13	18	75 - 100	65	52	-26	-41	25
14	16	75 - 100	170	173	94	98	-2
15	21	150 - 175	95	94	-42	-42	1
16	17	150 - 175	215	251	32	54	-14
17	23	75 - 100	110	83	26	-5	33
18	22	75 - 100	200	187	129	114	7
19	26	150 - 175	135	128	-17	-21	5
20	24	150 - 175	225	198	38	22	14
21	27	75 - 100	100	86	14	-2	16
22	25	75 - 100	180	178	106	103	1
23	28	150 - 175	100	121	-38	-26	-17
24	29	150 - 175	210	209	29	29	0
25	35	75 - 100	95	83	9	-5	14
26	31	75 - 100	190	191	117	118	-1
27	32	150 - 175	100	91	-38	-44	10
28	34	150 - 175	220	226	35	39	-3
29	30	75 - 100	85	97	-3	11	-12
30	37	75 - 100	195	213	123	143	-8
31	33	150 - 175	90	87	-45	-46	3
32	36	150 - 175	200	216	23	33	-7

Table 4.6: Measured slump according to CAC guidelines versus the measured slump using the traditional slump test and SLRM-II -Star points

Mix	Mix label	Slump (mm)			Difference (%)		
		CAC	Traditional test	SLRM-II	Slump test vs. CAC	SLRM-11 vs. CAC	Slump test vs. SLRM-11
33	55	75 - 100	200	183	129	109	9
34	52	25 - 50	140	142	273	279	-1
35	54	150 - 175	227	249	40	53	-9
36	57	75 - 100	210	194	140	122	8
37	51	75 - 100	195	195	123	123	0
38	60	25 - 50	175	180	367	380	-3
39	49	150 - 175	195	201	20	24	-3
40	58	75 - 100	210	174	140	99	21
41	47	125	190	190	52	52	0
42	48	125	190	188	52	50	1
43	62	125	185	180	48	44	3
44	63	125	190	196	52	57	-3
45	46	125	175	193	40	54	-9

concrete was used, one can still employ slump flow as a measure of workability. In this regard, three mathematical models that relate slump to slump flow were evaluated. They differ in the interpretation of the concrete geometry after it slumps. Chidiac et al. (2000) proposed that concrete maintains its conical shape and accordingly developed the following relationship

$$S_l = H - \frac{4V}{\pi\alpha S_f^2} = 0.3 - \frac{0.01}{S_f^2} \quad (4.1)$$

in which  $\alpha$  is a shape factor and for conical shape becomes 0.67. Kurokawa et al. (1994) developed a similar model with a shape factor of 0.58, where

$$S_l = H - \frac{12 * 10^{-3}}{S_f^2} = 0.3 - \frac{0.012}{S_f^2} \quad (4.2)$$

On the other hand, Domone (1998) assumed that the concrete slumps in a conical shape but the top diameter of the cone remains unchanged during slumping, where

$$S_l = H - \frac{12V(S_f - d)}{\pi(S_f^3 - d^3)} = 0.3 - \frac{0.021(S_f - 0.1)}{S_f^3 - 0.1^3} \quad (4.3)$$

where  $d(m)$  is the top diameter of the slump cone. Plots of the experimental data and calculated slump flow as a function of slump are shown in Figure 4.5. One observes that the model proposed by Chidiac et al. (2000) provides an excellent correlation with the experimental data up to the slump value of 200 mm. For a slump value greater than 200 mm, the other two models provide better correlation to the experimental data. The adequacy of the models was also investigated by determining the coefficient of determination,  $R^2$ . This quantity indicates the amount of variability explained by the analysis. All three models are found to have  $R^2$  more than 0.95 which suggest that 95% of the original variability of the measured data has been explained.

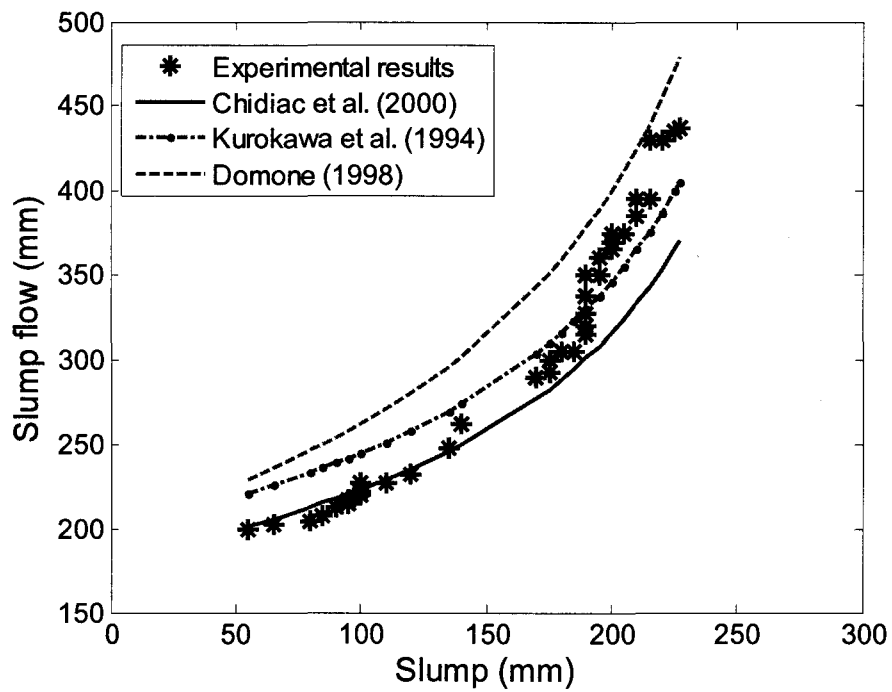


Figure 4.5: Comparison between experimental results and slump flow predicting models

### 4.2.3 Compressive Strength

The 28-day compressive strength of the concrete was evaluated in accordance with CSA test method A23.2-9C (CSA, 2000) and the results in the form of average and standard deviation are given in Tables 4.7 and 4.8. Moreover, the design compressive strength according to CAC guidelines are also given in Tables 4.7 and 4.8. One observes that the design strength is lower than the mean value with exception of Mix #38. These results indicate that the design strength according to CAC is adequate for controlling the compressive strength in mix design.

## 4.3 Regression Models

The method of least squares regression was used in analyzing and deriving the regression models. Coefficients of the model were estimated by minimizing the sum squares of the difference between the observed values and the predicted values from the model. The variables values were normalized to be consistent with the design values of CAC method for proportioning concrete mixture. The range of values adopted to normalize the models variables and the corresponding model input values are given in Table 4.9.

While developing the regression models, effects of the main variables and interaction of two variables were considered. Linear and nonlinear functions were also evaluated to describe the effects on the response. Best fit model was based on balancing between high correlation coefficient and low covariance. This approach permits one to develop models with low noise and high accuracy for predicting new observations. After selecting the best fit models, the significance of the model coefficients was checked using the t-test method. A probability value less than 5% was considered as significant evidence that the parameter is not zero and that it has a significant effect on the relevant response. The derived coefficients for the slump, slump flow, 28-day

Table 4.7: Measured compressive strength according to CAC guidelines versus the measured compressive strength -Main points

Mix	Mix label	28-day compressive strength (MPa)			
		Design value (CAC)	Measured strength		
			Average	Difference (%)	Standard deviation
1	44	34	38	11	2.27
2	42	20	23	16	1.21
3	38	34	36	7	0.98
4	43	20	26	29	2.65
5	40	34	36	5	1.83
6	45	20	24	20	2.04
7	39	34	38	13	1.40
8	41	20	24	19	2.33
9	19	34	41	21	1.99
10	14	20	28	38	0.33
11	20	34	43	25	3.59
12	15	20	28	41	0.20
13	18	34	40	18	1.73
14	16	20	28	41	0.86
15	21	34	35	3	1.19
16	17	20	30	50	0.76
17	23	34	41	21	1.30
18	22	20	24	19	0.83
19	26	34	37	8	2.77
20	24	20	28	38	1.58
21	27	34	37	10	0.93
22	25	20	26	29	1.01
23	28	34	36	6	2.29
24	29	20	26	30	1.07
25	35	34	41	19	1.24
26	31	20	29	46	0.74
27	32	34	41	20	1.81
28	34	20	30	51	1.07
29	30	34	36	7	0.83
30	37	20	28	42	0.85
31	33	34	40	19	1.27
32	36	20	28	38	1.97

Table 4.8: Measured compressive strength according to CAC guidelines versus the measured compressive strength -Star points

Mix	Mix label	28-day compressive strength (MPa)			
		Design value (CAC)	Measured strength		
			Average	Difference (%)	Standard deviation
33	55	26	30	17	0.77
34	52	15	15	0	0.75
35	54	26	33	27	1.03
36	57	15	18	23	0.67
37	51	26	31	18	2.58
38	60	15	14	-9	0.56
39	49	26	33	25	0.15
40	58	15	17	15	2.73
41	47	26	33	27	1.14
42	48	26	31	21	2.14
43	62	26	26	1	0.97
44	63	26	26	0	1.25
45	46	26	32	23	2.04



Table 4.9: Normalizing and model input ranges

	w/c		Water (kg/m <sup>3</sup> )		CA Size (mm)		SF %		Slag %		CA Volume	
<b>Normalizing range</b>	0.3	0.7	168	205	14	20	0	8	0	40	0.45	0.69
<b>Model input range</b>	-1	1	-1	1	-1	1	-1	1	-1	1	-1	1

compressive strength, yield stress and plastic viscosity models and their correlation coefficient are summarized in Table 4.10. These results show that more than 95% of the mixes results have been accounted for in the models. The corresponding regression models are:

$$Slump (mm) = 140.59 + 49.08 * water - 10.77 * SF + 93.61 * \log(1 + w/c) \quad (4.4)$$

$$Slump Flow (mm) = 294.6 + 127.81 * w/c + 60.07 * water - 15.44 * SF \\ + 54.1 * (w/c * water) - 98.12 * (w/c)^2 \quad (4.5)$$

$$Strength (MPa) = 33.55 - 11.99 * w/c + 1.6 * water + 1.91 * SF + 2.56 * CA \\ + 1.39 * (w/c * size) + 3.38 * (size * CA) - 7.78 * (CA)^2 \quad (4.6)$$

$$Yield Stress (Pa) = 1355.44 - 403.12 * water + 112.85 * SF - 252.66 * (w/c * size) \\ - 147.25 * (w/c * SF) - 90.49 * (size * SF) - 1168.58 * \log(1 + w/c) \quad (4.7)$$

$$Viscosity-1 (Pa.s) = 32.18 - 19.26 * water + 3.61 * SF - 9.85 * (w/c * SF) \\ - 3.69 * (size * SF) - 47.32 * \log(1 + w/c) \quad (4.8)$$

$$Viscosity-2 (Pa.s) = 29.24 - 13.45 * water + 2.66 * SF + 2.88 * CA \\ - 2.59 * (size * SF) - 25.1 * \log(1 + w/c) \quad (4.9)$$

Table 4.10: Coefficients of regression models

	Slump (mm)	Slump flow (mm)	f'c (28 days) MPa	Slump Rate Machine-II		
				Yield Stress (Pa)	Plastic Viscosity (Pa.s)	
					Chidiac Model	Proposed Model
<b>R<sup>2</sup></b>	<b>0.95</b>	<b>0.95</b>	<b>0.98</b>	<b>0.97</b>	<b>0.96</b>	<b>0.95</b>
<b>Equation</b>	<b>4.4</b>	<b>4.5</b>	<b>4.6</b>	<b>4.7</b>	<b>4.8</b>	<b>4.9</b>
intercept	140.59	294.60	33.55	1355.44	32.18	29.24
w/c	NS	127.81	-11.99	NS	NS	NS
water	49.08	60.07	1.60	-403.12	-19.26	-13.45
CA size	NS	NS	NS	NS	NS	NS
SF	-10.77	-15.44	1.91	112.85	3.61	2.66
Slag	NS	NS	NS	NS	NS	NS
CA content	NS	NS	2.56	NS	NS	2.88
w/c*water	NS	54.10	NS	NS	NS	NS
w/c*size	NS	NS	1.39	-252.66	NS	NS
w/c*SF	NS	NS	NS	-147.25	-9.85	NS
w/c*Slag	NS	NS	NS	NS	NS	NS
w/c*CA	NS	NS	NS	NS	NS	NS
w/c <sup>2</sup>	NS	-98.12	NS	NS	NS	NS
water*size	NS	NS	NS	NS	NS	NS
water*SF	NS	NS	NS	NS	NS	NS
water*Slag	NS	NS	NS	NS	NS	NS
water*CA	NS	NS	NS	NS	NS	NS
water <sup>2</sup>	NS	NS	NS	NS	NS	NS
size*SF	NS	NS	NS	-90.49	-3.69	-2.59
size*Slag	NS	NS	NS	NS	NS	NS
size*CA	NS	NS	3.38	NS	NS	NS
SF*Slag	NS	NS	NS	NS	NS	NS
SF*CA	NS	NS	NS	NS	NS	NS
Slag*CA	NS	NS	NS	NS	NS	NS
CA <sup>2</sup>	NS	NS	-7.78	NS	NS	NS
w/c <sup>3</sup>	NS	NS	NS	NS	NS	NS
water <sup>3</sup>	NS	NS	NS	NS	NS	NS
CA <sup>3</sup>	NS	NS	NS	NS	NS	NS
log(1+w/c)	93.61	NS	NS	-1168.58	-47.32	-25.10

\* NS-Not significant

## 4.4 Models Validation

The regression models were validated using four mixes that were not part of the experimental data used to develop the models. Validation of the results revealed that the maximum absolute error in predicting the slump, slump flow, compressive strength, yield stress, plastic viscosity model 1 and model 2 are 20 mm, 50 mm, 1.1 MPa, 94 Pa, 6.5 Pa.s, and 7 Pa.s, respectively. The measured versus the predicted properties corresponding to the test points as well as the main and star points are shown in Figures 4.6 to 4.11. The figures also display the standard error of the models with 95% confidence level (dotted lines). These results indicate that the models developed for slump, compressive strength and yield stress have predictions that are within the 95% confidence level, while the models of slump flow and plastic viscosity predictions have yielded less accuracy. The results demonstrates that the slump flow and plastic viscosity measurements have higher variability in comparison to the slump, strength and yield stress measurements.

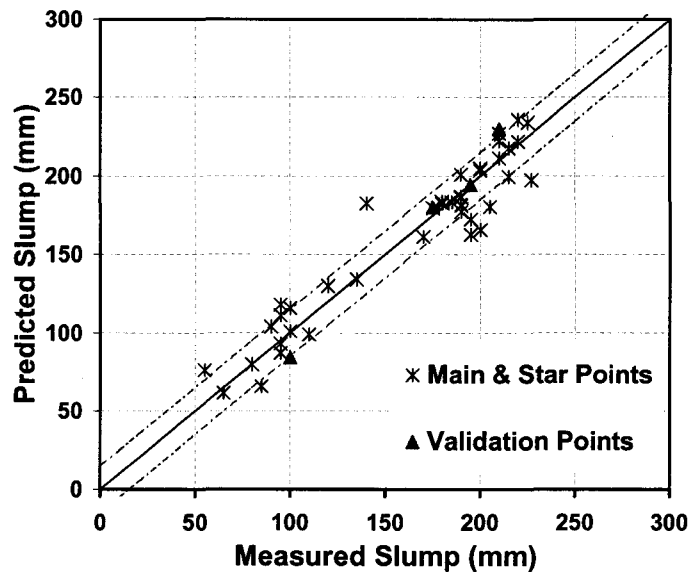


Figure 4.6: Measured slump versus predicted slump (Eq. 4.4)

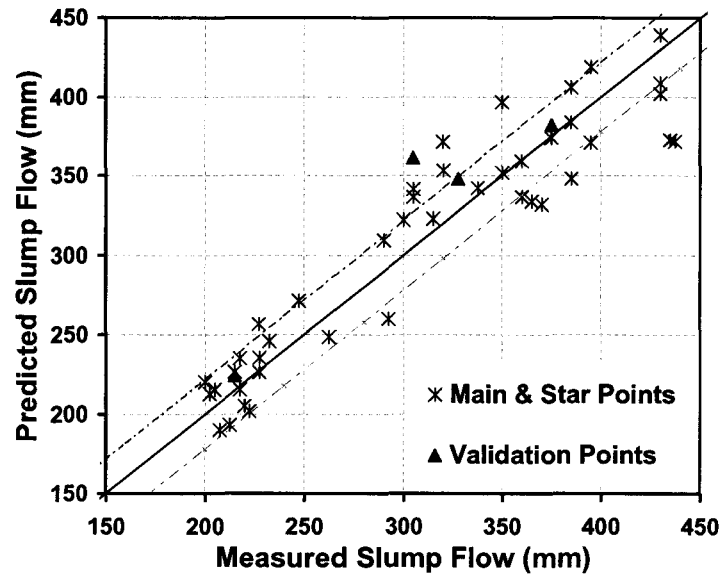


Figure 4.7: Measured slump flow versus predicted slump flow (Eq. 4.5)

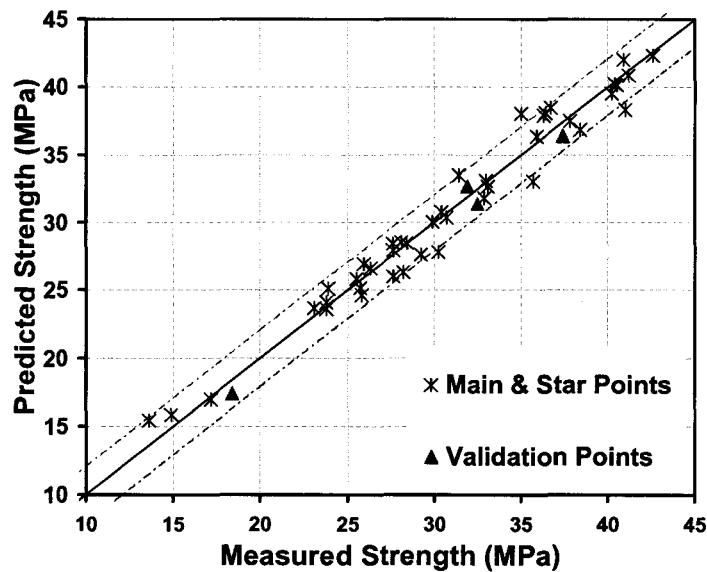


Figure 4.8: Measured compressive strength versus predicted compressive strength (Eq. 4.6)

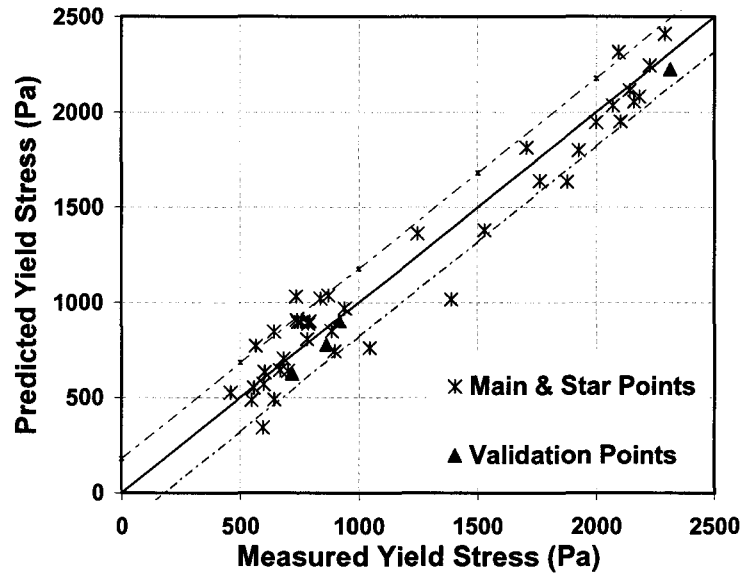


Figure 4.9: Estimated yield stress (Eq. 2.6) versus predicted yield stress (Eq. 4.7)

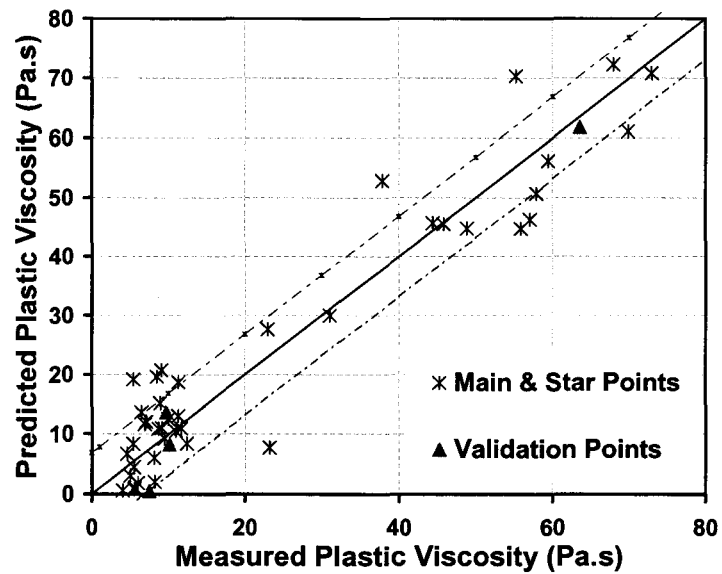


Figure 4.10: Estimated plastic viscosity (Eq. 2.9) versus predicted plastic viscosity (Eq. 4.8)

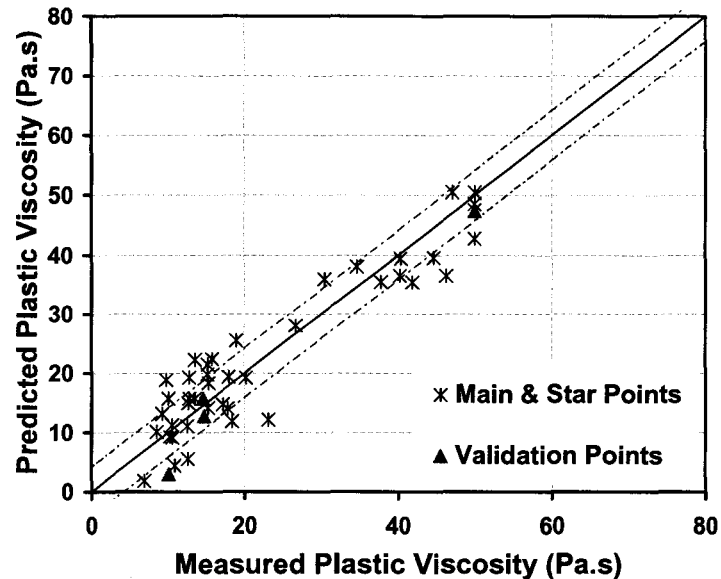


Figure 4.11: Estimated plastic viscosity (Eq. 2.8) versus predicted plastic viscosity (Eq. 4.9)

## 4.5 Models Evaluation

Mathematical models are useful tools for studying the influence of variables on relevant responses. In this study, the models are used to study the influence of the concrete mixtures on the properties of fresh concrete and the compressive strength.

### 4.5.1 Slump and Slump flow

From the slump model (Eq. 4.4), the variation of slump is found to be linear for water content and percent addition of silica fume and logarithmic for  $w/c$ . The model shows that increasing  $w/c$  and water content increases the slump, while increasing the silica fume will lead to a decrease in the slump. These trends are consistent with experimental observations. Furthermore, when comparing to CAC guidelines, it is found that current guidelines do not take into account  $w/c$  or percent addition of silica fume when designing for workability. CAC postulates that workability is only

a function of water content and maximum aggregate size. To study the effects of w/c on slump, the slump measurements were plotted against water content in Figure 4.12. One observes that water content is not a sufficient measure for slump. In comparison, a plot of computed slump values versus water content for different values of w/c is shown in Figures 4.13 and 4.14. Figure 4.13 displays the water content versus slump for maximum aggregate size of 14 mm and coarse aggregate content of 0.56. While Figure 4.14 shows the trends for maximum aggregate size of 20 mm and coarse aggregate content of 0.63. The results from the model display the same trends as found in Figure 4.12 and clearly show the effect of w/c on the slump. By plotting the corresponding slump values as postulated by CSA, one observes that they correspond to concrete mixtures with w/c of 0.4. Figure 4.15 displays the slump model predictions for varying w/c values as well as the measured slump. One observes that the model predictions have captured the measured value.

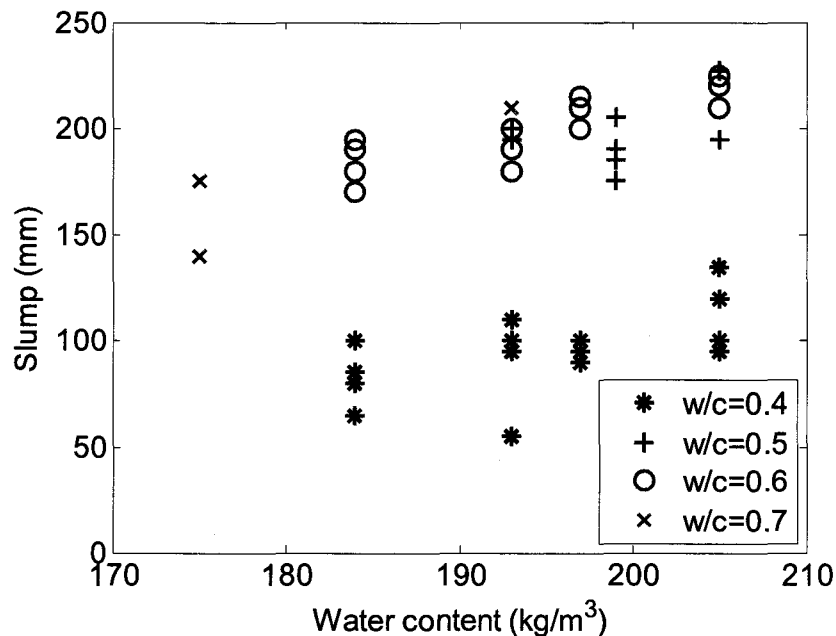


Figure 4.12: Water content versus slump measurements

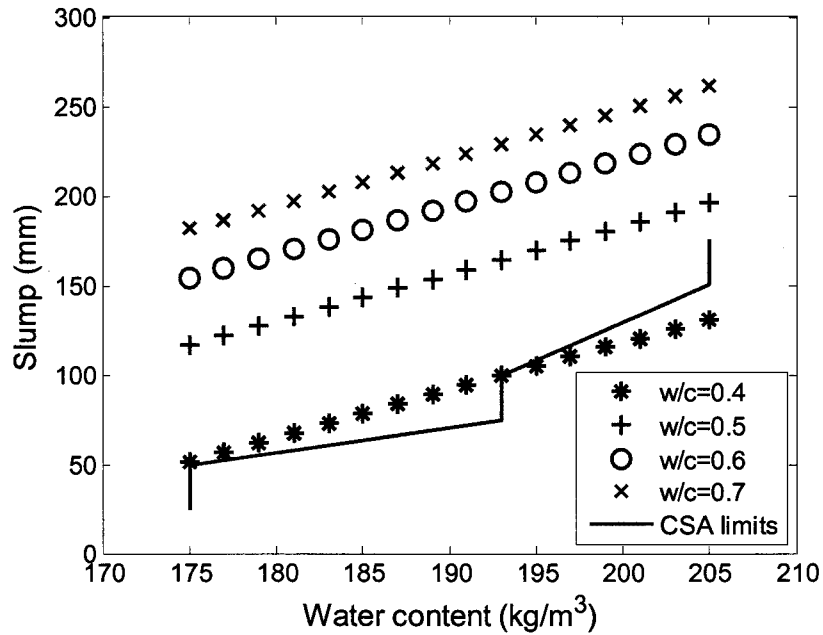


Figure 4.13: Water content versus slump for various levels of w/c; SF=0%, Slag=0%, Size=14mm and CA=0.56

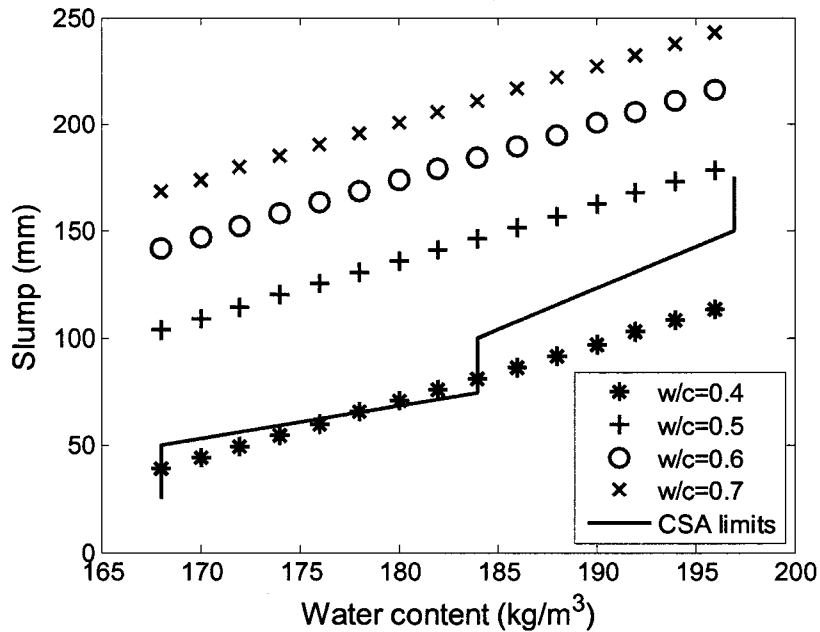


Figure 4.14: Water content versus slump for various levels of w/c; SF=0%, Slag=0%, Size=20mm and CA=0.63



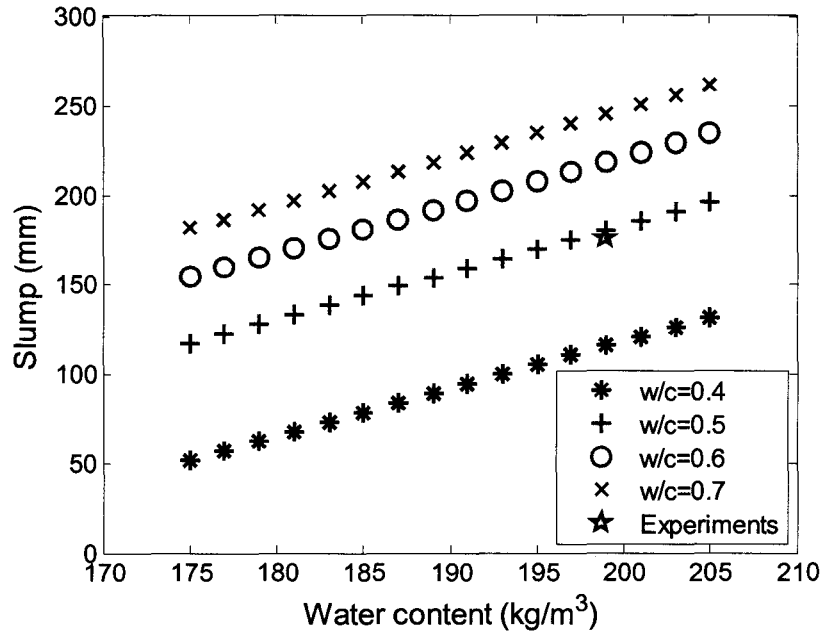


Figure 4.15: Measured and computed slump values versus water content for various levels of  $w/c$ ;  $SF=0\%$ ,  $Slag=0\%$ ,  $Size=14mm$ ,  $CA=0.56$  and  $w/c=0.5$

Regarding the slump flow, the derived regression model shows that it is affected by the  $w/c$ , water content, percent addition of silica fume, and the interaction between  $w/c$  and water content. The influence of  $w/c$  has been shown to vary in a quadratic manner. Closer examination of the model shows that by increasing the  $w/c$  and water content the slump flow increases, and by increasing the percent addition of silica fume the slump flow decreases. This trend is again consistent with experimental observations.

To study the effect of  $w/c$  on the slump flow, the measured slump flow values were plotted against water content in Figure 4.16. A plot of computed slump flow values versus water content for different values of  $w/c$  is shown in Figures 4.17 and 4.18. Figure 4.17 displays the water content versus slump flow for maximum aggregate size of 14 mm and coarse aggregate content of 0.56. While Figure 4.18 shows the trends for maximum aggregate size of 20 mm and coarse aggregate content of 0.63.

These figures show the complex relation between slump flow and concrete mixture and demonstrate that the current practice is too simplistic to provide an adequate design and control of fresh concrete workability.

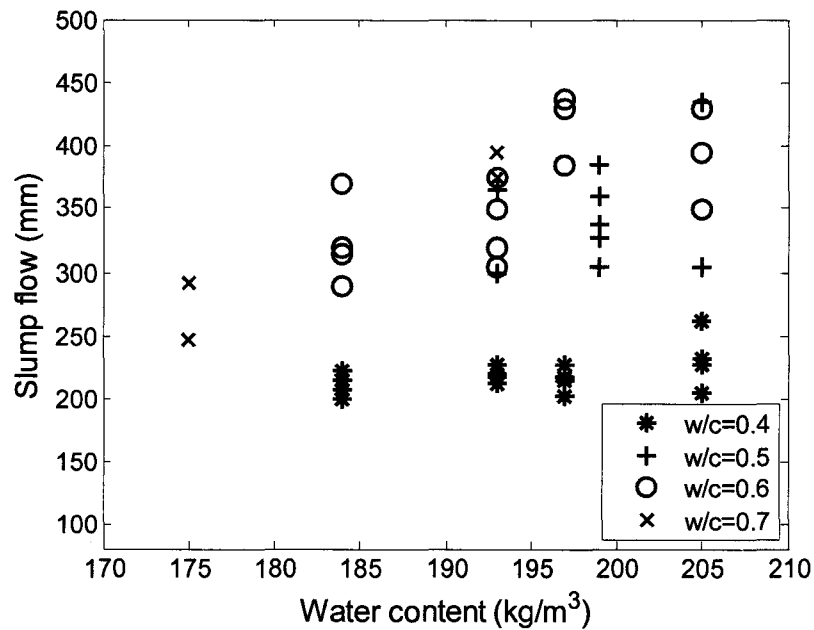


Figure 4.16: Water content versus slump flow measurements

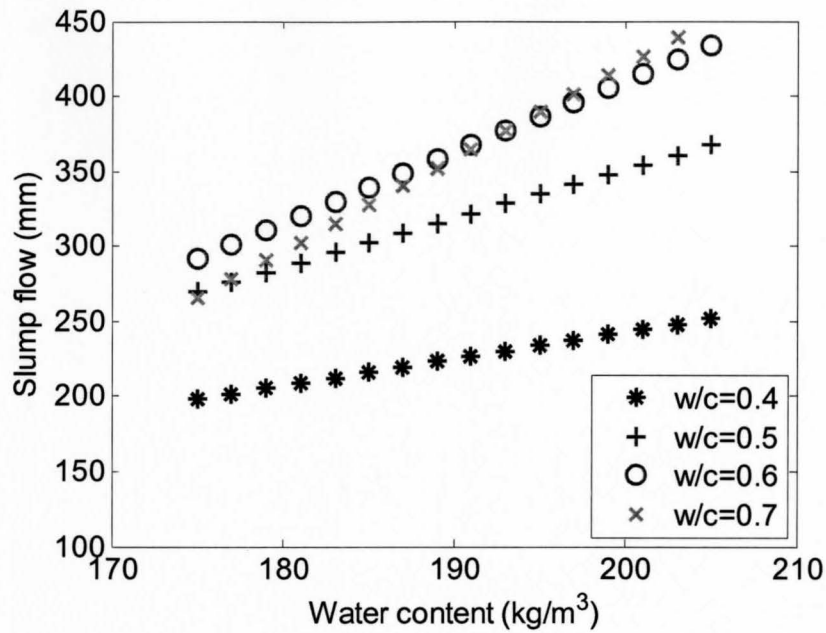


Figure 4.17: Water content versus slump flow for various levels of w/c; SF=0%, Slag=0%, Size=14mm and CA=0.56

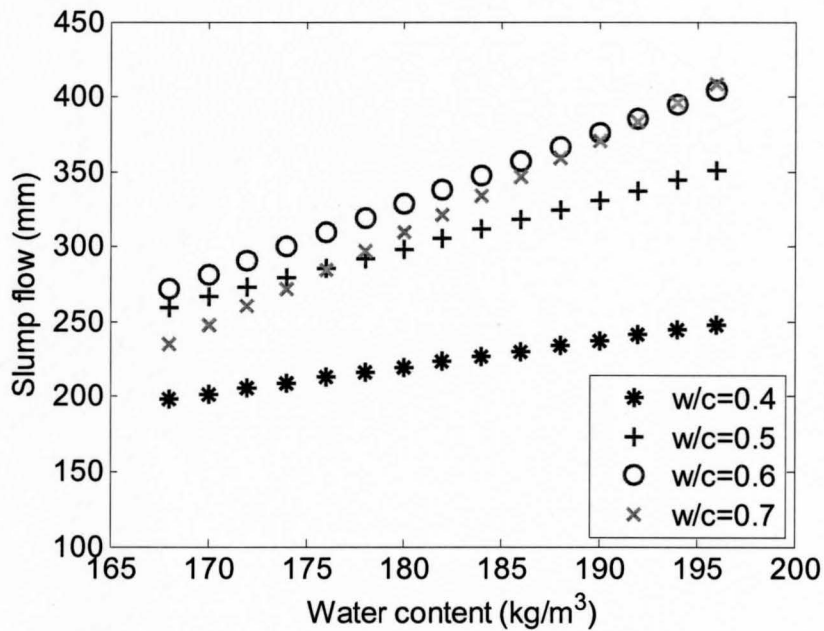


Figure 4.18: Water content versus slump flow for various levels of w/c; SF=0%, Slag=0%, Size=20mm and CA=0.63

### 4.5.2 Compressive strength

The model derived for the 28-day compressive strength of concrete is found to be strongly dependent on w/c given the magnitude of the coefficients in comparison to the other variables, namely water content, percent addition of silica fume and coarse aggregate content. Of interest is that the maximum aggregate size is found to be significant when it interacts with w/c and coarse aggregate content. Closer examination of the model shows that by increasing the w/c the strength decreases, and by increasing the amount of water and percent addition of silica fume the strength increases. These trends are consistent with experimental observations. The model also shows a complex relation between strength and the aggregate properties, namely maximum size and content. One can also examine the model predictions by plotting the predicted values to those suggested by CAC and the measured values as in Figure 4.19. The results indicate that the model predictions and those of CAC are acceptable and that the CAC design values for most mixes are conservative.

### 4.5.3 Yield stress

The regression model revealed that the yield stress is affected by w/c, water content, percent addition of silica fume, interaction between w/c and maximum aggregate size, interaction between w/c and percent addition of silica fume, and between maximum aggregate size and percent addition of silica fume. The influence of w/c has also been shown to vary in a logarithmic manner. Closer examination of the model reveals that yield stress increases when silica fume was added and decreases when water content or w/c increases. This trend is consistent with experimental observations. Figure 4.20 which shows a plot of yield stress versus water content, also illustrates the significance of water content and w/c on the yield stress. One observes that the model predictions have captured the measured value.

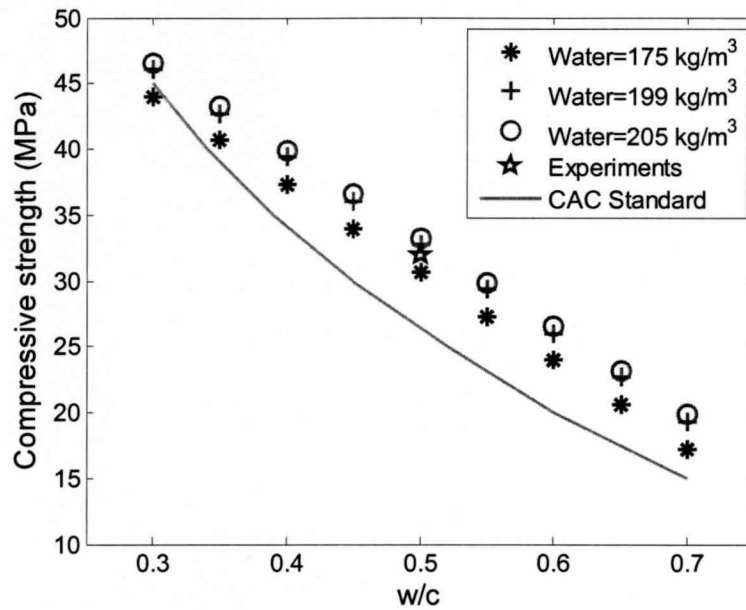


Figure 4.19: w/c versus 28-day compressive strength; SF=0%, Slag=0%, Size=14 mm, CA=0.56 and water content= 199 kg/m<sup>3</sup>

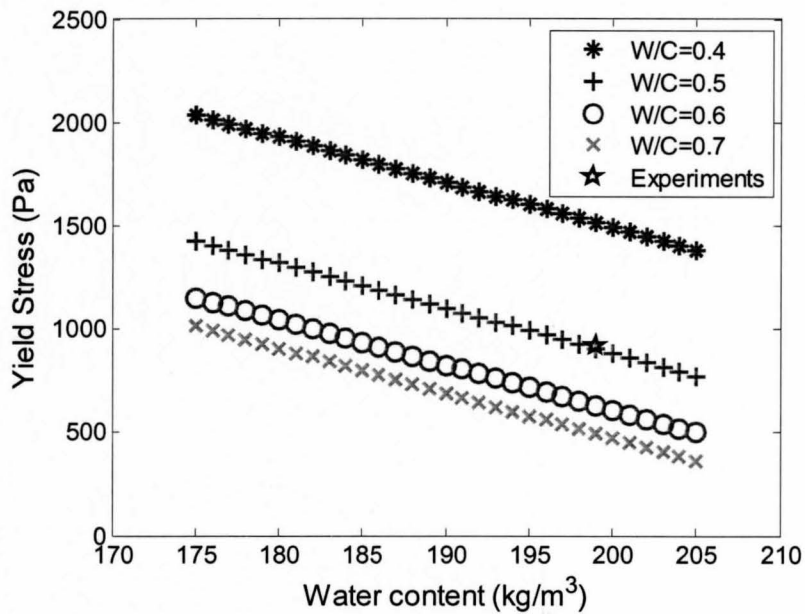


Figure 4.20: Predicted yield stress according to Eq. 2.6 and regression model versus water content for various levels of w/c; SF=0%, Slag=0%, Size=14mm, CA=0.56 and w/c=0.5

#### 4.5.4 Plastic viscosity

The regression model has revealed a complex relation between plastic viscosity and mix design variables. Plastic viscosity is found to be affected by w/c, water content, percent addition of silica fume, coarse aggregate content and the interaction between the maximum aggregate size and percent addition of silica fume. Increasing the w/c and water content results in a decrease in the plastic viscosity, while increasing the silica fume and coarse aggregate content results in an increase in the plastic viscosity. Relation between w/c and plastic viscosity is shown in Figure 4.21. The results show that four mixes with different w/c and water content can possess the same plastic viscosity. To discriminate between the concrete mixes, one needs to use both yield stress and plastic viscosity as shown in Figures 4.21 and 4.22.

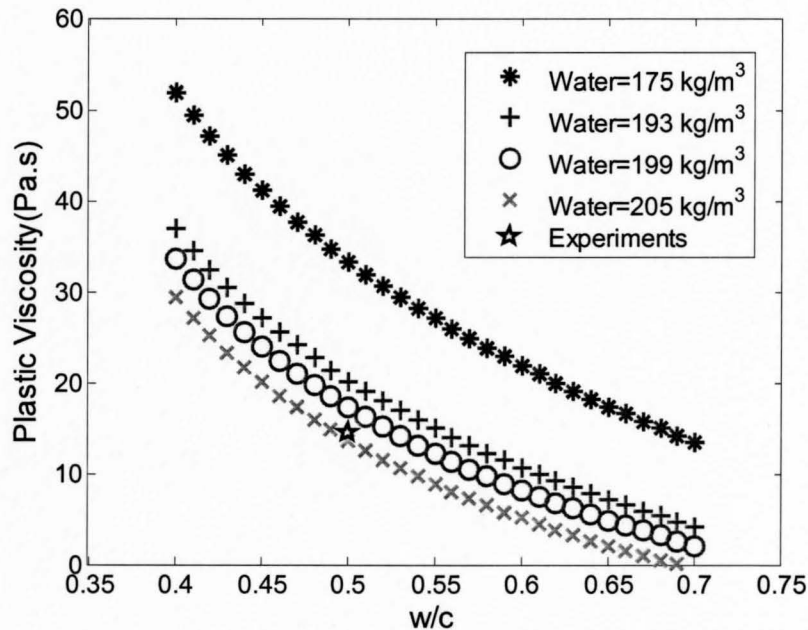


Figure 4.21: Effect of w/c on plastic viscosity for various levels of water; SF=0%, Slag=0%, Size=14mm, CA=0.56 and water content= 199 kg/m<sup>3</sup>

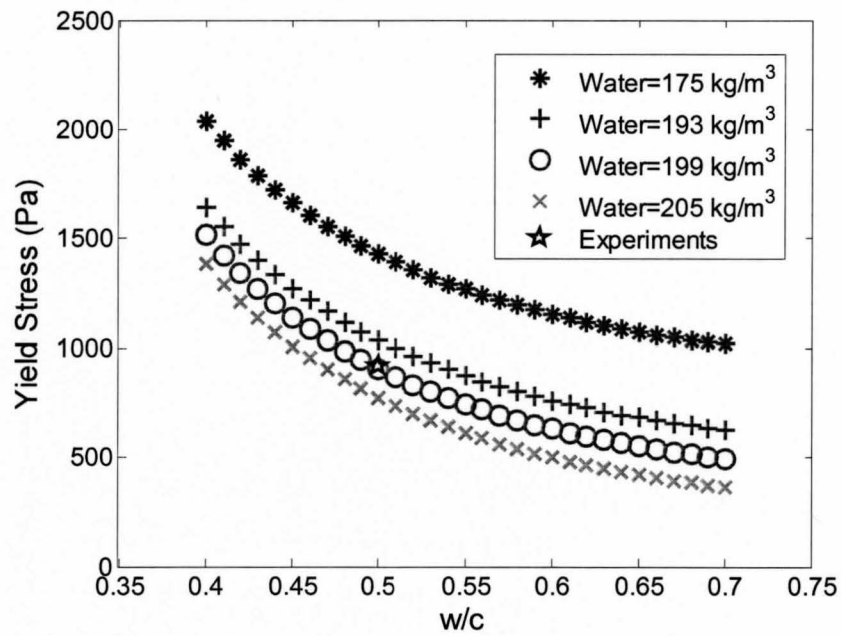


Figure 4.22: Effect of w/c on yield stress for various levels of water; SF=0%, Slag=0%, Size=14mm, CA=0.56 and water content= 199 kg/m<sup>3</sup>

# Chapter 5

## Concrete Mix Design

Cement Association of Canada (CAC) guidelines for proportioning concrete mixes do not account for the rheological properties of concrete. Such approach has been shown to be deficient in characterizing the flow behaviour of fresh concrete (Tattersall and Banfill, 1983). In this chapter, the Neuro-Fuzzy technique is proposed as a useful method for correlating concrete mix design to the rheological properties, namely yield stress and plastic viscosity. This approach will permit the inclusion of the rheological properties in the concrete mix design. Neuro-Fuzzy refers to applying Neural-Network learning technique to optimize fuzzy logic parameters (Nayaka et al., 2004, Xiong et al., 2001). Different learning technique and different types of fuzzy interface system (FIS) have been presented in the literature (Jang et al., 1993, Jang et al., 1995, Nayaka et al., 2004, Xiong et al., 2001). In this research, the model reported by Jang et al., (1993), referred to as Adaptive Network Based Fuzzy Interface System (ANFIS), has been adopted to correlate the current mixture proportioning standard to the rheological properties of concrete. The network was constructed using the experimental data reported in Chapter 3 and Chapter 4. The correlation is intended for determining the mix design ingredients, namely w/c, water content, fine aggregate content and coarse aggregate content that will yield concrete with the



following properties; compressive strength, yield stress and plastic viscosity.

This chapter consists of three sections. The first section provides an introduction to the Neuro-Fuzzy technique and a brief description of the type of fuzzy interface system. The application of the Neuro-Fuzzy method to correlate concrete mix design to the rheological properties of concrete and compressive strength is presented in Section two. The statistical significance of each design target on the mixture proportions was evaluated using the t-test method. Subsequently, the Neuro-Fuzzy was trained using the experimental results. Section three presents a comparative evaluation of the two design methods Neuro-Fuzzy method and CAC method.

## 5.1 Neuro-fuzzy model

Neuro-Fuzzy refers to applying Neural-Network learning technique to optimize fuzzy logic parameters (Nayaka et al., 2004, Xiong et al., 2001). There are many types and techniques of fuzzy interface system. The model reported by Jang et al., (1993, 1995), referred to as Adaptive Network Based Fuzzy Interface System (ANFIS) which is based on Sugeno fuzzy model and shown in Figure 5.1 (Jang et al., 1993, Jang et al., 1995), has been used in this project.

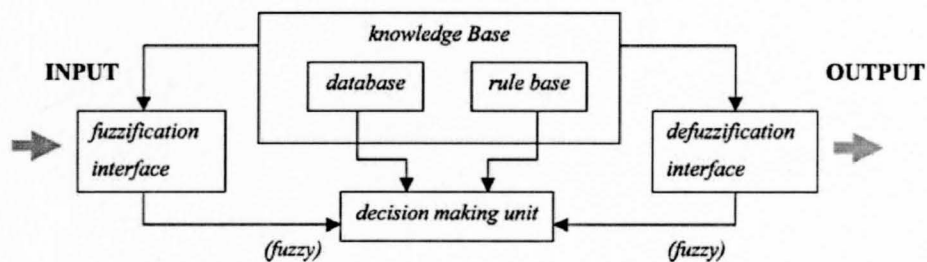


Figure 5.1: Fuzzy interface system chart (Nayaka et al., 2004, Jang et al., 1993)

ANFIS is a five layer feed forward network with two type of modifiable parameters; membership function (MF) parameters which have a nonlinear relation with output,

and the consequent parameters (rules parameters) which have a linear relation with output. Therefore, the learning process is a hybrid method consisting of gradient descent algorithms for nonlinear part and linear least square method for the linear part. For illustration, Figure 5.2 shows the function associated with each layer. The first layer is “fuzzification” in which the membership grades to each linguistic label, such as low or high, are found based on the crisp inputs. To define the linguistic label, different membership functions can be used such as Triangular, Generalized Bell, Gaussian and Gaussian combination which are shown in Figure 5.3. Such functions have different number of parameters as given below:

Triangular-shape:

$$\mu(x) = \begin{cases} 0 & x \leq a \\ \frac{x-a}{b-a} & a \leq x \leq b \\ \frac{c-x}{c-b} & b \leq x \leq c \\ 0 & c \leq x. \end{cases}$$

Generalized bell-shaped:

$$\mu(x) = \frac{1}{1 + \left| \frac{x-c}{a} \right|^{2b}}$$

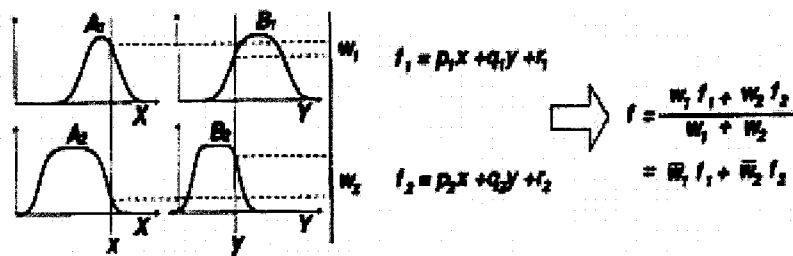
Gaussian:

$$\mu(x) = \exp\left(-\frac{(x-c)^2}{2\sigma^2}\right)$$

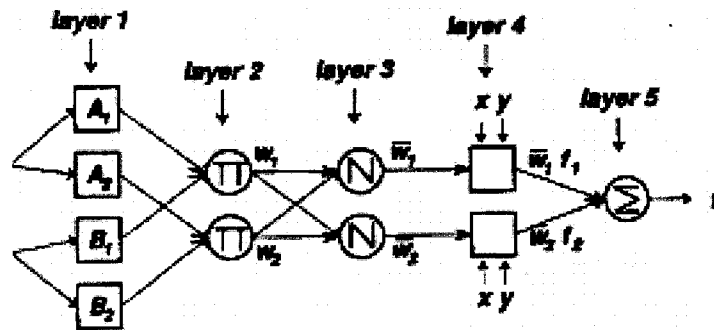
Gaussian combination:

$$\mu(x) = \begin{cases} \exp\left(-\frac{(x-c_1)^2}{2\sigma_1^2}\right) & x < c_1 \\ 1 & c_2 \leq x \leq c_1 \\ \exp\left(-\frac{(x-c_2)^2}{2\sigma_2^2}\right) & c_2 < x. \end{cases}$$

In the second and third layers, the firing strength of each rule is computed and normalized. While in the fourth layer, the output of each layer is calculated based on the input and normalized firing strength. Finally, the overall output is calculated



(a)



(b)

Figure 5.2: (a) Sugeno fuzzy model, (b) Equivalent ANFIS architecture (Nayaka et al., 2004, Jang et al., 1993)

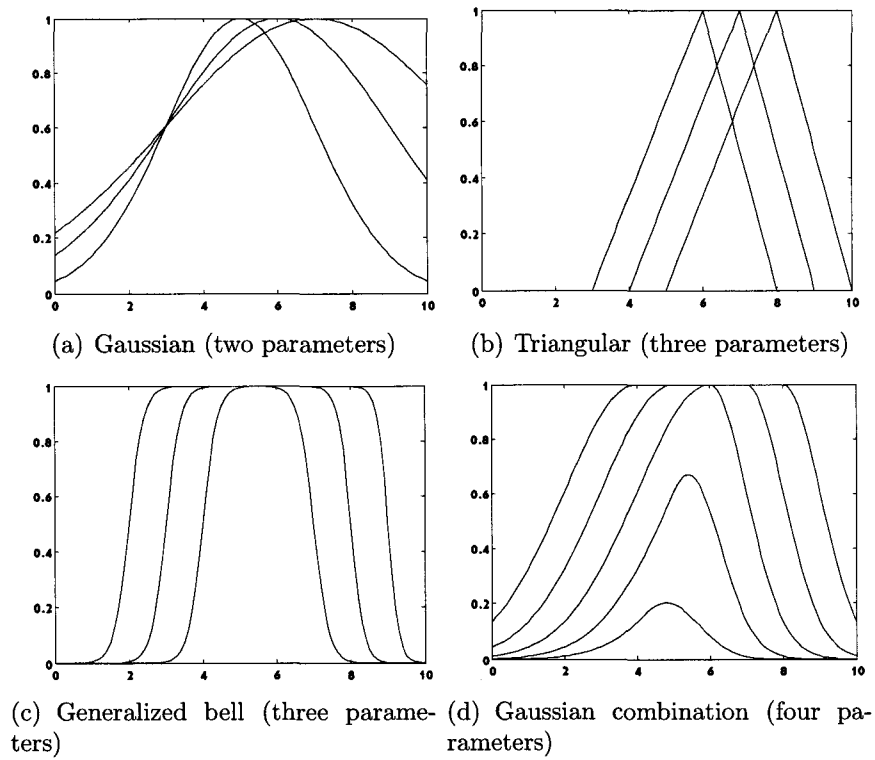


Figure 5.3: Different membership functions

in the last layer. As shown in Figure 5.2, the consequent part of this FIS is linear; therefore there is no need for "defuzzification". It should be noted that the number of data points has to be considered in selecting the type of membership function and the number of linguistic label and rules (Nayaka et al., 2004, Takagi et al., 1985, Jang et al., 1993, Xiong et al., 2001).

## 5.2 ANFIS Model

In general, Neuro-Fuzzy network requires a large number of data points to train the parameters. As a result, it is not feasible to consider all the design targets, namely compressive strength, yield stress and plastic viscosity for predicting concrete mix ingredients. Therefore, statistical methods, specifically the least squares regression and t-test, have been used to first evaluate the statistical significance of the mix design parameters; w/c , water content and bulk volume of coarse aggregate. Recognizing that the sample size consists of 45 mixes, additional design constraints were added to the model. These include the maximum aggregate size and addition of mineral admixtures. Accordingly, the structure of the model is shown in Figure 5.4.

In the t-test, probability less than 10% was considered as significant evidence that the coefficient is not zero and it has significant effect on the response. The significance of the compressive strength, yield stress and plastic viscosity have been checked with regard to mix design parameters; w/c, water content and bulk volume of coarse aggregate. The corresponding coefficients are given in Table 5.1. The results show that the compressive strength, yield stress and silica fume have significant effect on the w/c, while the compressive strength and yield stress have significant effect on the water content. Finally, the compressive strength and plastic viscosity have significant effect on the bulk volume of coarse aggregate. Such results imply that the cement content and water content in concrete mixtures are affected mainly by

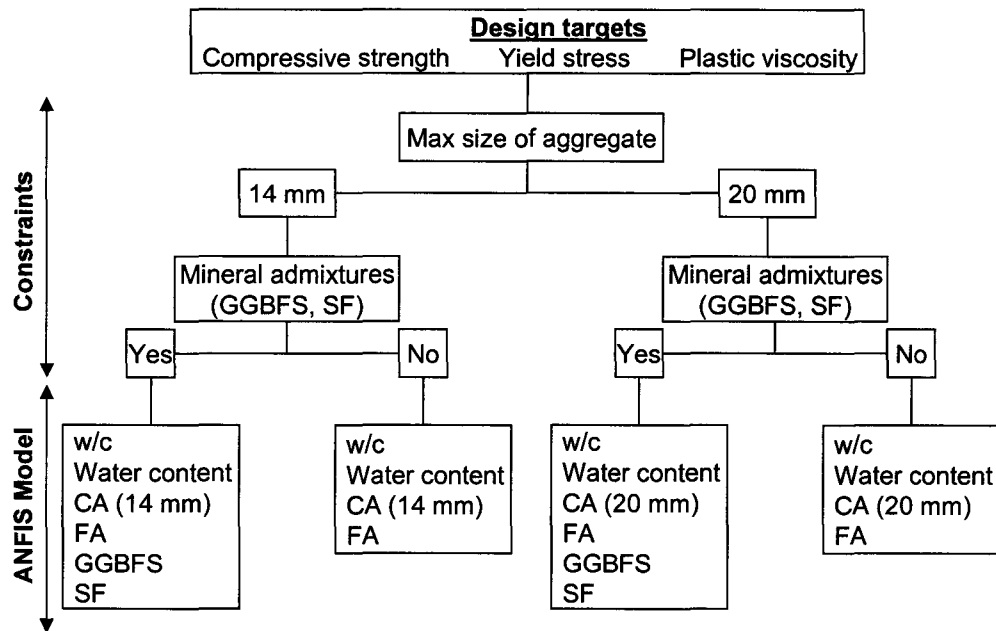


Figure 5.4: Schematic illustration of the model decision making process

compressive strength and yield stress. On the other side, the required fine to coarse aggregate content is mainly affected by the compressive strength and plastic viscosity.

Table 5.1: Coefficients corresponding to w/c, water content and bulk volume of coarse aggregate derived from t-test

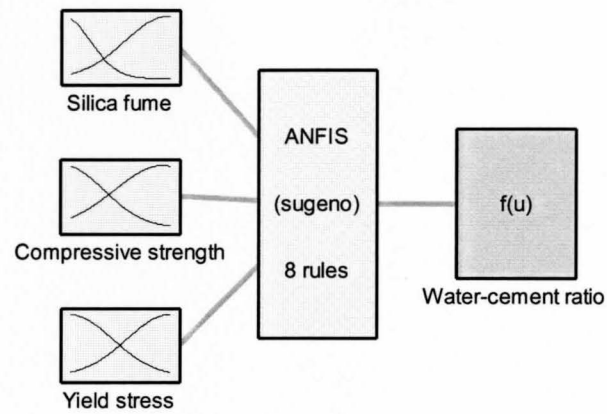
	w/c	Water content (kg/m <sup>3</sup> )	Coarse aggregate bulk volume
<b>R<sup>2</sup></b>	<b>0.97</b>	<b>0.75</b>	<b>0.62</b>
<b>intercept</b>	0.55	189.27	0.600
<b>Compressive strength</b>	-0.17	14.52	-0.013
<b>Yield stress</b>	-0.06	-9.03	NS
<b>Plastic viscosity</b>	NS	NS	0.143

### 5.2.1 Training the ANFIS model to predict the mix design

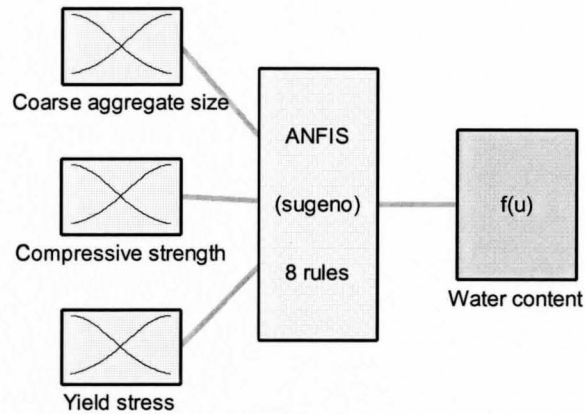
According to the t-test results, the ANFIS model was trained to predict the w/c from the compressive strength and yield stress, and to predict the water content from

the compressive strength and yield stress, and to predict the bulk volume of coarse aggregate from the compressive strength and plastic viscosity. Notwithstanding the fact that the training also includes the constraints noted in Figure 5.4. The results of compressive strength, yield stress and plastic viscosity for the 45 experimental mixes have been used in training the model. The general structure of the ANFIS model for w/c, water content and bulk volume of coarse aggregate is shown in Figure 5.5.

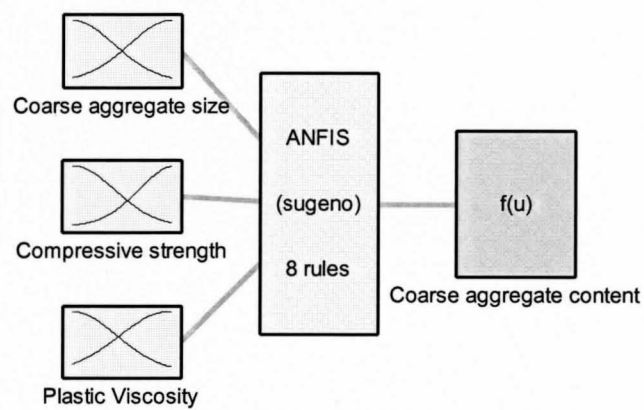
Two linguistic labels, low and high, were defined for each input. Gaussian function with two parameters was used as a membership function and the consequent part of the FIS is assumed constant. The linguistics labels for the inputs are illustrated in Figure 5.6. The adequacy of the model is evaluated by comparing the model predictions with the experimental data as shown in Figures 5.7 to 5.9 corresponding to w/c, water content and bulk volume of coarse aggregate. As shown in the figures, the model has yielded good predictions for the w/c with less accuracy for the water content and coarse aggregate. It is apparent that more experimental data are needed to train the ANFIS.



(a)



(b)



(c)

Figure 5.5: General structure of ANFIS model for (a) water-cement ratio; (b) water content; (c) bulk volume of coarse aggregate



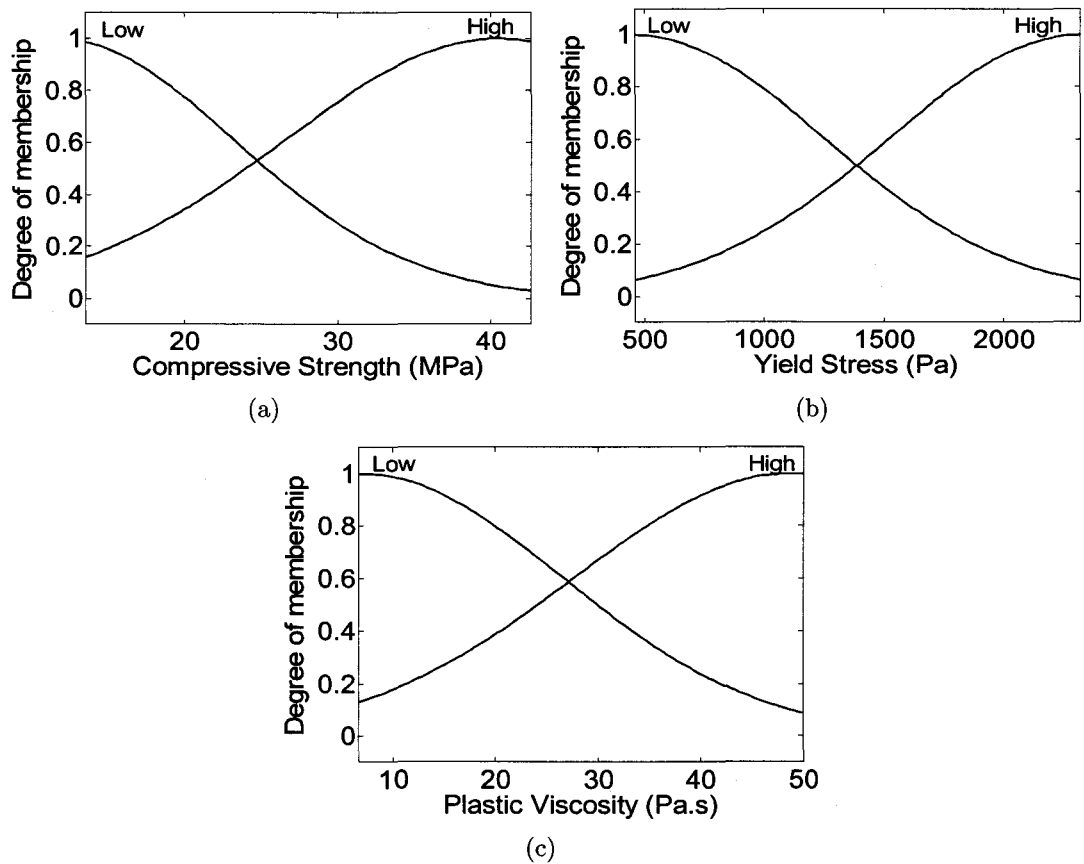


Figure 5.6: Degree of membership for (a) Compressive Strength; (b) Yield Stress; (c) Plastic Viscosity - Partitioning to low and high

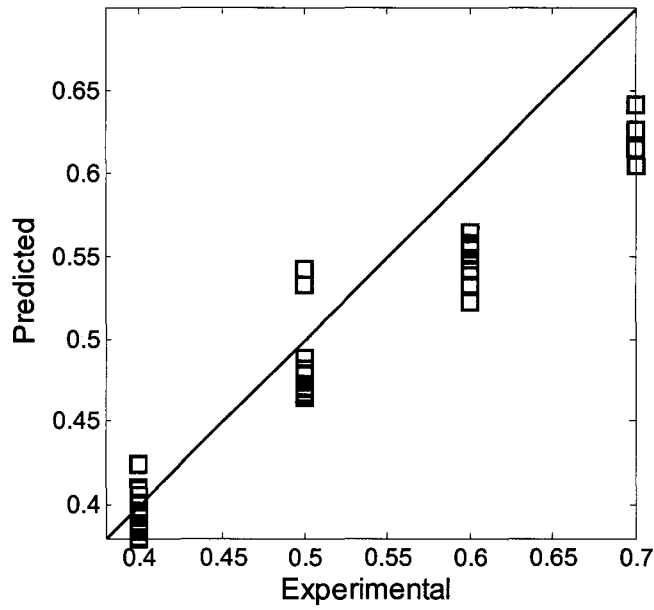


Figure 5.7: Model prediction versus experimental data for water-cement ratio

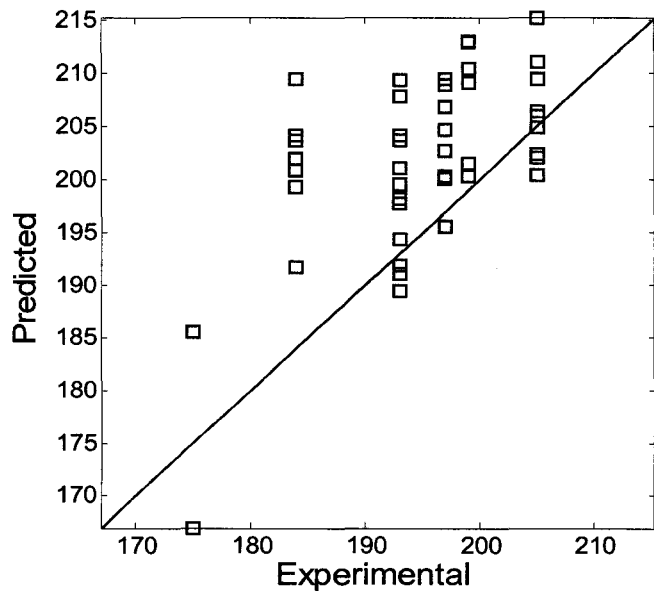


Figure 5.8: Model prediction versus experimental data for water content

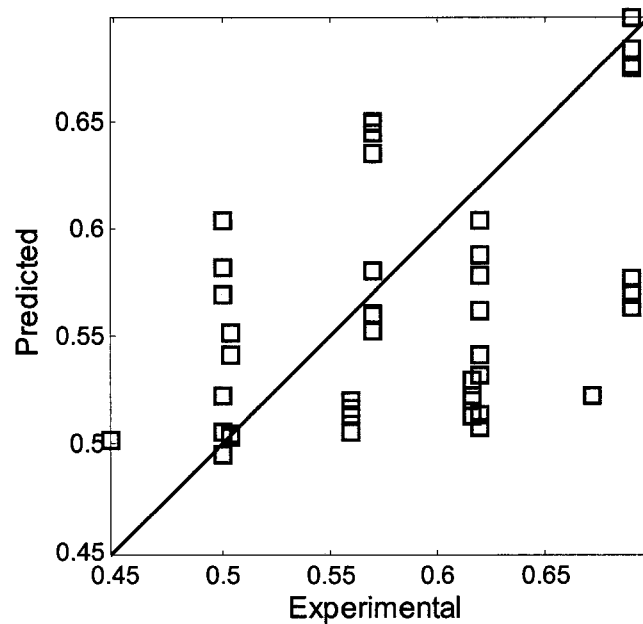


Figure 5.9: Model prediction versus experimental data for bulk volume of coarse aggregate

### 5.2.2 Derived rules for the mix design from the ANFIS model

After training the ANFIS model, rules for each output corresponding to the mix design parameters, were derived. The rules for the water-cement ratio are:

1. If percent addition of silica fume is low, compressive strength is low and yield stress is low, then water-cement ratio is 0.69.
2. If percent addition of silica fume is low, compressive strength is low and yield stress is high, then water-cement ratio is 0.6.
3. If percent addition of silica fume is low, compressive strength is high and yield stress is low, then water-cement ratio is 0.43.
4. If percent addition of silica fume is low, compressive strength is high and yield stress is high, then water-cement ratio is 0.35.

5. If percent addition of silica fume is high, compressive strength is low and yield stress is low, then water-cement ratio is 0.71.
6. If percent addition of silica fume is high, compressive strength is low and yield stress is high, then water-cement ratio is 0.62.
7. If percent addition of silica fume is high, compressive strength is high and yield stress is low, then water-cement ratio is 0.49.
8. If percent addition of silica fume is high, compressive strength is high and yield stress is high, then water-cement ratio is 0.36.

The rules of water content are:

1. If aggregate size is 14 mm, compressive strength is low and yield stress is low, then water content is  $193 \text{ kg/m}^3$ .
2. If aggregate size is 14 mm, compressive strength is low and yield stress is high, then water content is  $134 \text{ kg/m}^3$ .
3. If aggregate size is 14 mm, compressive strength is high and yield stress is low, then water content is  $228 \text{ kg/m}^3$ .
4. If aggregate size is 14 mm, compressive strength is high and yield stress is high, then water content is  $200 \text{ kg/m}^3$ .
5. If aggregate size is 20 mm, compressive strength is low and yield stress is low, then water content is  $185 \text{ kg/m}^3$ .
6. If aggregate size is 20 mm, compressive strength is low and yield stress is high, then water content is  $131 \text{ kg/m}^3$ .
7. If aggregate size is 20 mm, compressive strength is high and yield stress is low, then water content is  $230 \text{ kg/m}^3$ .

8. If aggregate size is 20 mm, compressive strength is high and yield stress is high, the water content is  $216 \text{ kg/m}^3$ .

The rules of bulk volume of coarse aggregate are:

1. If aggregate size is 14 mm, compressive strength is low and plastic viscosity is low, then bulk volume of coarse aggregate is 0.44.
2. If aggregate size is 14 mm, compressive strength is low and plastic viscosity is high, then bulk volume of coarse aggregate is 0.68.
3. If aggregate size is 14 mm, compressive strength is high and plastic viscosity is low, then bulk volume of coarse aggregate is 0.49.
4. If aggregate size is 14 mm, compressive strength is high and plastic viscosity is high, then bulk volume of coarse aggregate is 0.62.
5. If aggregate size is 20 mm, compressive strength is low and plastic viscosity is low, then bulk volume of coarse aggregate is 0.49.
6. If aggregate size is 20 mm, compressive strength is low and plastic viscosity is high, then bulk volume of coarse aggregate is 0.74.
7. If aggregate size is 20 mm, compressive strength is high and plastic viscosity is low, then bulk volume of coarse aggregate is 0.55.
8. If aggregate size is 20 mm, compressive strength is high and plastic viscosity is high, then bulk volume of coarse aggregate is 0.67.

Tables 5.2 - 5.4 provide a summary of the derived rules. The rules predict the mix design according to the definition of low and high values for each input.

Table 5.2: Rules derived for the water-cement ratio from the results of the network

	<b>Silica Fume</b>							
	0 %				8 %			
	<b>Compressive Strength</b>				<b>Compressive Strength</b>			
	Low		High		Low		High	
	<b>Yield Stress</b>		<b>Yield Stress</b>		<b>Yield Stress</b>		<b>Yield Stress</b>	
	Low	High	Low	High	Low	High	Low	High
w/c	0.69	0.60	0.43	0.35	0.71	0.62	0.49	0.36

Table 5.3: Rules derived for the water content from the results of the network

	<b>Maximum aggregate size</b>							
	14 mm				20 mm			
	<b>Compressive Strength</b>				<b>Compressive Strength</b>			
	Low		High		Low		High	
	<b>Yield Stress</b>		<b>Yield Stress</b>		<b>Yield Stress</b>		<b>Yield Stress</b>	
	Low	High	Low	High	Low	High	Low	High
Water content (kg/m <sup>3</sup> )	193	134	228	200	185	131	230	216

Table 5.4: Rules derived for the bulk volume of coarse aggregate from the results of the network

	<b>Maximum aggregate size</b>							
	14 mm				20 mm			
	<b>Compressive Strength</b>				<b>Compressive Strength</b>			
	Low		High		Low		High	
	<b>Plastic Viscosity</b>		<b>Plastic Viscosity</b>		<b>Plastic Viscosity</b>		<b>Plastic Viscosity</b>	
	Low	High	Low	High	Low	High	Low	High
Coarse aggregate Bulk volume	0.44	0.68	0.49	0.62	0.49	0.74	0.55	0.67

### 5.3 Concrete Mix Design based on the Neuro-Fuzzy method

The derived rules of the Neuro-Fuzzy model can be used to calculate the three mix design parameters, namely w/c, water content and bulk volume of coarse aggregate, using the three input parameters, namely compressive strength, yield stress and plastic viscosity in addition to the two constraints coarse aggregate size and mineral admixtures. To define the steps for proportioning concrete mixes using this method, guidelines for the method have been plotted in Figure 5.10. As shown in the figure, the water-cement ratio is determined from the required strength, yield stress, which indicates the slump value and affected by adding silica fume to the mix. While the water content is determined from the compressive strength, yield stress and the coarse aggregate size. The coarse aggregate content is determined from the compressive strength, plastic viscosity and coarse aggregate size. These steps are different than the ones in the method of Cement Association of Canada (CAC), which are shown in Figure 2.1, where the w/c is determined just from the strength, and the water content from the slump and coarse aggregate size, while the coarse aggregate content is determined from the aggregate size.

To evaluate for designing concrete mixtures, a comparative study was carried out between the developed method and that of Cement Association of Canada. Mixture proportions for 72 concrete mixes with different design targets of slump, strength and plastic viscosity, and with different constraints size of aggregate and mineral admixtures, were developed and are given in Tables 5.5 and 5.6. It should be noted that the yield stress was calculated from the slump flow using Eq. 2.6. Slump flow was calculated from the target slump using Eq. 4.1. The concrete is assumed to have a density of 2400 kg/m<sup>3</sup>.

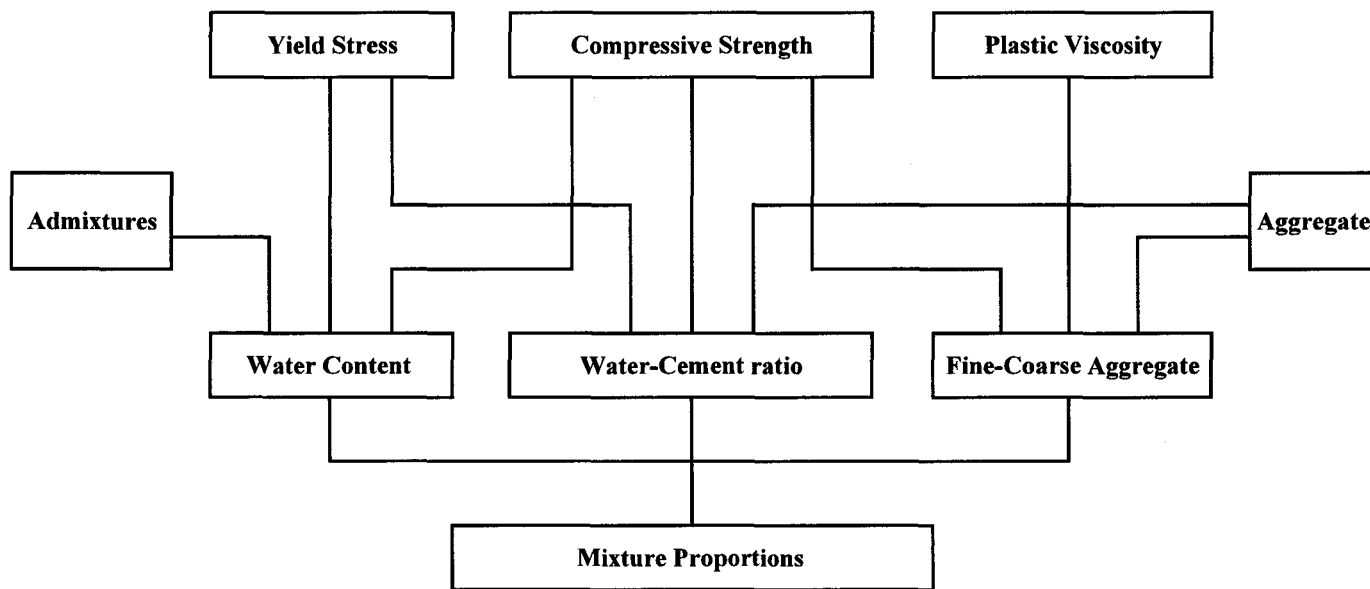


Figure 5.10: Guidelines for proportioning concrete mixes using Neuro-Fuzzy method



Table 5.5: Design targets with no mineral admixtures

Mix	Design targets				Constraints		
	Strength (MPa)	Slump (mm)	Yield stress (Pa)	Viscosity (Pa.s)	Coarse aggregate size (mm)	Mineral admixtures	
						Silica fume (%)	Slag (%)
1		75	2144	Low	14	0	0
2				High	14	0	0
3	15	150	1429	Low	14	0	0
4				High	14	0	0
5		200	953	Low	14	0	0
6				High	14	0	0
7		75	2144	Low	14	0	0
8				High	14	0	0
9	25	150	1429	Low	14	0	0
10				High	14	0	0
11		200	953	Low	14	0	0
12				High	14	0	0
13		75	2144	Low	14	0	0
14				High	14	0	0
15	35	150	1429	Low	14	0	0
16				High	14	0	0
17		200	953	Low	14	0	0
18				High	14	0	0
19		75	2144	Low	20	0	0
20				High	20	0	0
21	15	150	1429	Low	20	0	0
22				High	20	0	0
23		200	953	Low	20	0	0
24				High	20	0	0
25		75	2144	Low	20	0	0
26				High	20	0	0
27	25	150	1429	Low	20	0	0
28				High	20	0	0
29		200	953	Low	20	0	0
30				High	20	0	0
31		75	2144	Low	20	0	0
32				High	20	0	0
33	35	150	1429	Low	20	0	0
34				High	20	0	0
35		200	953	Low	20	0	0
36				High	20	0	0

Table 5.6: Design targets with mineral admixtures

Mix	Design targets				Constraints		
	Strength	Slump	Yield stress	Viscosity	Coarse aggregate size (mm)	Mineral admixtures	
	(MPa)	(mm)	(Pa)	(Pa.s)		Silica fume (%)	Slag (%)
37				Low	14	8	0
38		75	2144	High	14	8	0
39	15			Low	14	8	0
40		150	1429	High	14	8	0
41				Low	14	8	0
42		200	953	High	14	8	0
43				Low	14	8	0
44		75	2144	High	14	8	0
45	25			Low	14	8	0
46		150	1429	High	14	8	0
47				Low	14	8	0
48		200	953	High	14	8	0
49				Low	14	8	0
50		75	2144	High	14	8	0
51	35			Low	14	8	0
52		150	1429	High	14	8	0
53				Low	14	8	0
54		200	953	High	14	8	0
55				Low	20	8	0
56		75	2144	High	20	8	0
57	15			Low	20	8	0
58		150	1429	High	20	8	0
59				Low	20	8	0
60		200	953	High	20	8	0
61				Low	20	8	0
62		75	2144	High	20	8	0
63	25			Low	20	8	0
64		150	1429	High	20	8	0
65				Low	20	8	0
66		200	953	High	20	8	0
67				Low	20	8	0
68		75	2144	High	20	8	0
69	35			Low	20	8	0
70		150	1429	High	20	8	0
71				Low	20	8	0
72		200	953	High	20	8	0

The concrete mixtures were proportioned following the Neuro-Fuzzy method and the CAC method for the purpose of comparison and the results are given in Tables 5.7 and 5.8. As expected, CAC design method does not account for the plastic viscosity. In comparison, the Neuro-Fuzzy method modifies the coarse aggregate bulk volume to account for the high and low viscosity. Another obvious observation is the addition of mineral admixtures. CAC method does not take into account the properties of mineral admixtures and therefore yields the same mixture proportions regardless of the amount of silica fume added. The w/c was modified by the Neuro-Fuzzy method when silica fume was added as cement replacement. Both design methods adjusted the w/c to account for the strength. However, when the slump or yield stress was changed, only the Neuro-Fuzzy method adjusted both the w/c and water content. CAC method only changed the water content to account for the change in slump or yield stress. These results indicate that a difference in the design philosophy of concrete mixture is needed to adequately design for the rheological properties of fresh concrete.

Table 5.7: Concrete mixtures following Neuro-Fuzzy method and CAC - mix design with no mineral admixtures

Mix	Mix design					
	Neuro-Fuzzy method			CAC method		
	w/c	Water content	CA	w/c	Water content	CA
1	0.58	148	0.44	0.70	193	0.56
2	0.58	148	0.68	0.70	193	0.56
3	0.61	172	0.44	0.70	205	0.56
4	0.61	172	0.68	0.70	205	0.56
5	0.63	186	0.44	0.70	213	0.56
6	0.63	186	0.68	0.70	213	0.56
7	0.49	166	0.465	0.52	193	0.56
8	0.49	166	0.65	0.52	193	0.56
9	0.52	185	0.465	0.52	205	0.56
10	0.52	185	0.65	0.52	205	0.56
11	0.54	197	0.465	0.52	213	0.56
12	0.54	197	0.65	0.52	213	0.56
13	0.40	192	0.49	0.39	193	0.56
14	0.40	192	0.62	0.39	193	0.56
15	0.43	206	0.49	0.39	205	0.56
16	0.43	206	0.62	0.39	205	0.56
17	0.45	215	0.49	0.39	213	0.56
18	0.45	215	0.62	0.39	213	0.56
19	0.58	146	0.49	0.70	184	0.63
20	0.58	146	0.74	0.70	184	0.63
21	0.61	167	0.49	0.70	197	0.63
22	0.61	167	0.74	0.70	197	0.63
23	0.63	180	0.49	0.70	206	0.63
24	0.63	180	0.74	0.70	206	0.63
25	0.49	168	0.52	0.52	184	0.63
26	0.49	168	0.705	0.52	184	0.63
27	0.52	184	0.52	0.52	197	0.63
28	0.52	184	0.705	0.52	197	0.63
29	0.54	195	0.52	0.52	206	0.63
30	0.54	195	0.705	0.52	206	0.63
31	0.40	201	0.55	0.39	184	0.63
32	0.40	201	0.67	0.39	184	0.63
33	0.43	211	0.55	0.39	197	0.63
34	0.43	211	0.67	0.39	197	0.63
35	0.45	217	0.55	0.39	206	0.63
36	0.45	217	0.67	0.39	206	0.63

Table 5.8: Concrete mixtures following Neuro-Fuzzy method and CAC - mix design with mineral admixtures

Mix	Mix design					
	Neuro-Fuzzy method			CAC method		
	w/c	Water content	CA	w/c	Water content	CA
37	0.59	148	0.44	0.7	193	0.56
38	0.59	148	0.68	0.7	193	0.56
39	0.63	172	0.44	0.7	205	0.56
40	0.63	172	0.68	0.70	205	0.56
41	0.66	186	0.44	0.70	213	0.56
42	0.66	186	0.68	0.70	213	0.56
43	0.51	166	0.465	0.52	193	0.56
44	0.51	166	0.65	0.52	193	0.56
45	0.55	185	0.465	0.52	205	0.56
46	0.55	185	0.65	0.52	205	0.56
47	0.58	197	0.465	0.52	213	0.56
48	0.58	197	0.65	0.52	213	0.56
49	0.42	192	0.49	0.39	193	0.56
50	0.42	192	0.62	0.39	193	0.56
51	0.47	206	0.49	0.39	205	0.56
52	0.47	206	0.62	0.39	205	0.56
53	0.50	215	0.49	0.39	213	0.56
54	0.50	215	0.62	0.39	213	0.56
55	0.59	146	0.49	0.70	184	0.63
56	0.59	146	0.74	0.70	184	0.63
57	0.63	167	0.49	0.70	197	0.63
58	0.63	167	0.74	0.70	197	0.63
59	0.66	180	0.49	0.70	206	0.63
60	0.66	180	0.74	0.70	206	0.63
61	0.51	168	0.52	0.52	184	0.63
62	0.51	168	0.705	0.52	184	0.63
63	0.55	184	0.52	0.52	197	0.63
64	0.55	184	0.705	0.52	197	0.63
65	0.58	195	0.52	0.52	206	0.63
66	0.58	195	0.705	0.52	206	0.63
67	0.42	201	0.55	0.39	184	0.63
68	0.42	201	0.67	0.39	184	0.63
69	0.47	211	0.55	0.39	197	0.63
70	0.47	211	0.67	0.39	197	0.63
71	0.50	217	0.55	0.39	206	0.63
72	0.50	217	0.67	0.39	206	0.63

To evaluate the merits of the two design methods, the regression model developed in the previous Chapter was used to calculate the properties based on the mixture proportions. The results are given in Table 5.9 and 5.10. A comparison of the 28-day compressive strength show that the Neuro-Fuzzy method yields values that are comparable to the design values where the maximum percent difference for the design is given in Table 5.11. The maximum percent error using the CAC method is found to be at least three times greater than that obtained using the Neuro-Fuzzy method. When examining the slump or yield stress, one observes that the slump values obtained using CAC method are arbitrary and do not reflect the specified design value. On the other side, the Neuro-Fuzzy method yields slump values that are consistent with the specified design slump and yield stress values. Lastly, when one examines the plastic viscosity values, only the Neuro-Fuzzy method yields values that are reasonable and comparable to the experimental data. CAC method doesn't account for the rheological properties and the results do support this hypothesis.

Table 5.9: Results of the Neuro-Fuzzy method and CAC - mix design with no mineral admixtures

Mix	Computed properties following							
	Neuro-Fuzzy method				CAC method			
	Strength (MPa)	Slump (mm)	Yield stress (Pa)	Viscosity (Pa.s)	Strength (MPa)	Slump (mm)	Yield stress (Pa)	Viscosity (Pa.s)
1	15.9	81	1765	38.1	18.8	229	624	4.2
2	15.1	74	1779	43.7	18.8	229	624	4.2
3	15.9	152	1202	20.2	19.8	261	362	1.0
4	15.1	145	1216	25.8	19.8	261	362	1.0
5	15.8	195	857	9.9	20.5	282	188	0.6
6	15.0	189	871	15.5	20.5	282	188	0.6
7	26.2	90	1661	39.2	30.8	173	963	17.9
8	26.0	85	1671	43.6	30.8	173	963	17.9
9	25.8	155	1125	21.1	31.9	205	701	9.4
10	25.7	150	1135	25.5	31.9	205	701	9.4
11	25.5	195	800	10.6	32.6	226	527	3.8
12	25.4	190	811	15.0	32.6	226	527	3.8
13	36.5	99	1655	35.8	39.5	89	1747	39.4
14	36.7	96	1662	38.8	39.5	89	1747	39.4
15	35.7	161	1105	18.2	40.6	121	1486	29.3
16	35.9	157	1112	21.3	40.6	121	1486	29.3
17	35.1	197	789	8.3	41.3	142	1311	22.6
18	35.3	194	796	11.4	41.3	142	1311	22.6
19	16.4	82	1760	43.5	20.5	211	466	13.3
20	15.1	75	1775	49.4	20.5	211	466	13.3
21	16.6	147	1168	26.9	21.7	246	183	6.6
22	15.3	140	1182	32.8	21.7	246	183	6.6
23	16.7	187	801	17.2	22.4	269	-	2.2
24	15.4	180	815	23.1	22.4	269	-	2.2
25	26.3	102	1788	41.8	30.1	155	1259	28.8
26	25.8	97	1798	46.1	30.1	155	1259	28.8
27	26.2	160	1242	25.9	31.2	190	976	19.6
28	25.6	155	1253	30.2	31.2	190	976	19.6
29	26.0	195	908	16.7	32.0	213	786	13.5
30	25.5	190	919	21.0	32.0	213	786	13.5
31	36.3	129	1863	32.6	37.0	72	2372	51.6
32	36.3	126	1870	35.5	37.0	72	2372	51.6
33	35.5	179	1334	18.9	38.1	106	2089	40.6
34	35.5	176	1341	21.7	38.1	106	2089	40.6
35	35.0	208	1028	11.3	38.9	129	1899	33.3
36	35.0	205	1035	14.1	38.9	129	1899	33.3

Table 5.10: Results of the Neuro-Fuzzy method and CAC - mix design with mineral admixtures

Mix	Computed properties following							
	Neuro-Fuzzy method				CAC method			
	Strength (MPa)	Slump (mm)	Yield stress (Pa)	Viscosity (Pa.s)	Strength (MPa)	Slump (mm)	Yield stress (Pa)	Viscosity (Pa.s)
37	19.1	62	1903	47.3	22.6	207	621	14.7
38	18.2	56	1916	52.9	22.6	207	621	14.7
39	18.4	136	1269	28.8	23.7	239	359	8.5
40	17.6	129	1283	34.4	23.7	239	359	8.5
41	17.6	182	871	18.2	24.4	261	185	4.4
42	16.8	175	885	23.8	24.4	261	185	4.4
43	28.6	78	1860	46.7	34.7	152	1224	28.4
44	28.5	73	1871	51.1	34.7	152	1224	28.4
45	27.6	146	1253	28.4	35.7	183	963	19.9
46	27.5	141	1264	32.7	35.7	183	963	19.9
47	26.7	188	873	17.7	36.4	205	789	14.3
48	26.5	183	884	22.1	36.4	205	789	14.3
49	39.0	95	1891	41.8	43.4	68	2200	49.9
50	39.2	91	1898	44.9	43.4	68	2200	49.9
51	36.9	164	1206	22.8	44.4	100	1939	39.8
52	37.1	161	1214	25.9	44.4	100	1939	39.8
53	35.6	203	844	13.1	45.1	121	1765	33.1
54	35.8	199	851	16.2	45.1	121	1765	33.1
55	19.7	63	1511	42.4	24.4	190	101	13.5
56	18.4	56	1525	48.2	24.4	190	101	13.5
57	19.4	131	822	25.0	25.5	224	-	6.8
58	18.1	124	837	30.9	25.5	224	-	6.8
59	18.9	174	377	15.0	26.2	247	-	2.3
60	17.6	167	391	20.9	26.2	247	-	2.3
61	29.1	90	1575	39.0	33.9	134	1159	29.0
62	28.6	85	1585	43.3	33.9	134	1159	29.0
63	28.4	150	933	22.7	35.0	168	876	19.8
64	27.9	145	943	27.1	35.0	168	876	19.8
65	27.7	188	518	13.3	35.8	191	686	13.6
66	27.2	183	529	17.6	35.8	191	686	13.6
67	39.1	125	1687	28.5	40.8	50	2464	51.7
68	39.0	122	1694	31.3	40.8	50	2464	51.7
69	37.2	183	973	13.4	41.9	85	2180	40.8
70	37.2	179	980	16.2	41.9	85	2180	40.8
71	36.1	214	595	5.8	42.7	108	1991	33.4
72	36.1	210	602	8.6	42.7	108	1991	33.4



Table 5.11: Maximum percent difference between calculated values and design values for compressive strength

Design Method	Percent of difference (%)							
	Neuro-Fuzzy method				CAC method			
Max aggregate size	14 mm		20 mm		14 mm		20 mm	
Silica fume	0%	8%	0%	8%	0%	8%	0%	8%
15 MPa	6	27	11	31	37	63	49	75
25 MPa	5	14	5	16	30	46	26	43
35 MPa	5	12	4	12	18	29	11	22

Figures 5.11 to 5.13 provide a comparison between the Neuro-Fuzzy method and CAC method in achieving the target design values for compressive strength, slump and yield stress, respectively. Again, results of Figure 5.11 indicate that the CAC method is too conservative with values that are for the most cases 25% greater than the design value when the silica fume was not added and 40% greater when the silica fume was added. Whereas the Neuro-Fuzzy method has yielded values that are for the most cases 6% higher where no mineral admixtures were added and 15% when silica fume was added. Results of Figure 5.12 indicate that the slump values obtained using the Neuro-Fuzzy method are within  $\pm 25$  mm tolerance specified for the slump test. Results from CAC show that the slump is either much greater or lower than the tolerated 25 mm. The same trend is observed for the yield stress. In brief, these results show that the CAC method provides a conservative mix design for the compressive strength and does not appear to yield any consistent values for the rheological properties. The Neuro-Fuzzy method has shown that higher control can be achieved in designing for compressive strength, yield stress and plastic viscosity. These results mean that a revision of the design guidelines is merited.

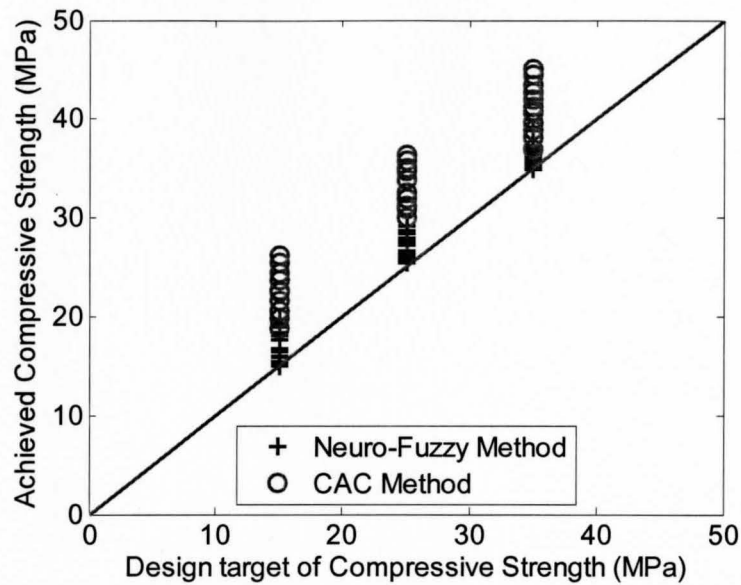


Figure 5.11: Design target of compressive strength versus achieved strength using Neuro-Fuzzy method and CAC standard method

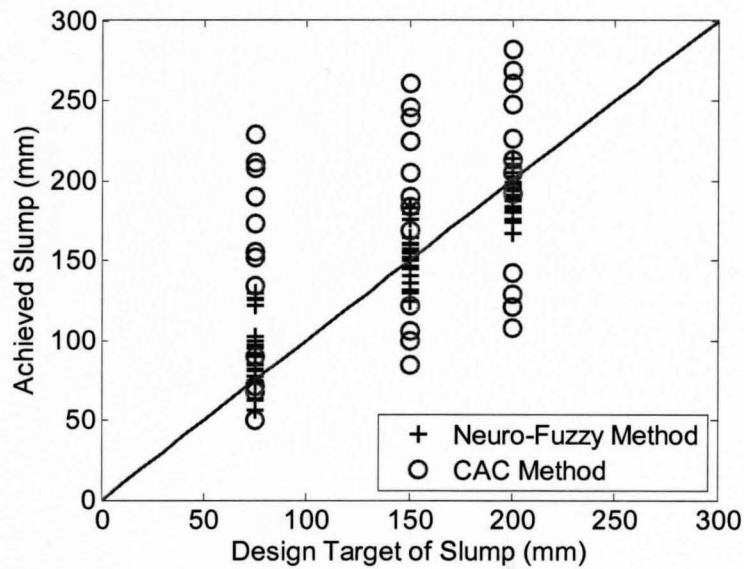


Figure 5.12: Design target of slump versus achieved slump using Neuro-Fuzzy method and CAC standard method

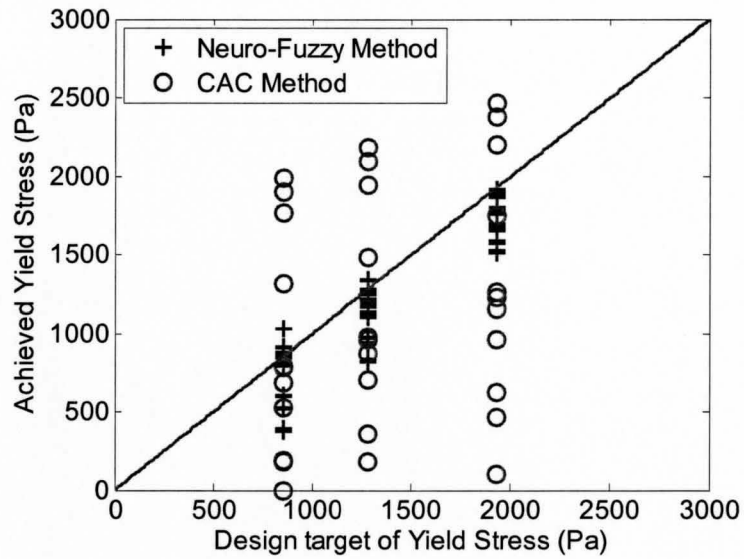


Figure 5.13: Design target of yield stress versus achieved yield stress using Neuro-Fuzzy method and CAC standard method

## Chapter 6

# Conclusions and Recommendations

The ability of current method of proportioning concrete mixes, in describing the flow behavior of fresh concrete and achieving the design targets, have been evaluated in this research. Such evaluation has been conducted using an experimental program developed using statistical models that are based on the factorial design method. 45 concrete mixtures were evaluated to measure their rheological properties and compressive strength. Statistical models were derived for slump, slump flow, compressive strength, yield stress and plastic viscosity based on the experimental results obtained from this study. Moreover, a Neuro-Fuzzy network was adopted to correlate the current mix design to the Bingham's rheological properties; yield stress and plastic viscosity and to the compressive strength. The results of experimental concrete mixes have been used to train and validate the network. Then, rules for calculating the mixture proportions, namely water-cement ratio, water content and fine to coarse aggregate from the compressive strength, yield stress and plastic viscosity have been derived from the network results. Such rules were used to design concrete mixes with different design targets. Concrete mixes were subsequently designed using the Neuro-Fuzzy and CAC standard design method. Mixes were then evaluated using the statistical models and the results were compared as an assessment of the design

methods to yield adequate concrete mixtures.

On the basis of the results obtained from this research, the following conclusions can be drawn:

1. Current design practices for concrete mixture proportioning are too simplistic for describing the flow behavior of fresh concrete including slump.
2. Slump which is a measure of yield stress, is not a sufficient measure for designing and controlling the workability of fresh concrete.
3. The Bingham's rheological properties, yield stress and plastic viscosity need to be incorporated into the design of concrete mixtures to improve its ability in describing the flow behavior.
4. The water-cement ratio has a significant effect on the fresh and hardened properties of concrete.
5. Current design practices for concrete mixture proportioning are not accurate in achieving the design target of slump, which indicates the yield stress, because it does not account for water-cement ratio.
6. Current design practices for concrete mixture proportioning do not account for the plastic viscosity in designing and controlling of fresh concrete mixes.
7. Current design practices for concrete mixture proportioning are too conservative in designing for compressive strength.
8. Deriving mathematical models based on the statistical factorial design is a useful method to understand the influence of concrete mixture proportions on concrete fresh and hardened properties.

9. The Slump rate machine is a convenient apparatus for determining the plastic viscosity of fresh concrete, and it does not require extensive training for operation.
10. Water-cement ratio and water content have a significant effect on the compressive strength and yield stress. Bulk volume of coarse aggregate has a significant effect on the plastic viscosity.
11. The required cement pasts in concrete mixture is affected mainly by compressive strength and yield stress. While, the required fine to coarse aggregate ratio is mainly affected by the plastic viscosity.
12. Adopting the Neuro-Fuzzy network to correlate current mix design to the rheological properties of concrete, is found to be adequate for determining the water content, cement content, fine and coarse aggregates from yield stress, plastic viscosity and compressive strength.
13. By adopting the Neuro-Fuzzy method for designing concrete mixes, two levels of plastic viscosity, low and high, were developed for mixes with the same slump and compressive strength.
14. Current design method for concrete mixture need to include the rheological properties, yield stress and plastic viscosity, in order to achieve the needed quality control for fresh concrete.

## 6.1 Recommendations

Based on the results from this study, one can recommend the followings:

1. Widen the experimental program to include non-entrained air mixes, self consolidating concrete, mixes with varying amount of mineral and chemical admixtures.
2. Modify the current concrete mix design guidelines to account for the rheological properties.
3. Need to introduce other workability test method such as the slump rate machine to adequately characterize the rheological properties of fresh concrete.

## References

- [1] ACI Committee 238, 2008, Report on measurements of workability and rheology of fresh concrete, ACI 238.1R-08, American Concrete Institute, Farmington Hills, MI, USA.
- [2] ACI Committee 318, 2005, Building Code Requirements for Structural Concrete and Commentary, ACI 318-05, American Concrete Institute, USA.
- [3] ACI, 1974, Proportioning Concrete Mixes, Publication SP-46, American Concrete Institute, Detroit.
- [4] BASF, The Chemical Company “Admixture For Improving Concrete” ,Master Builders, 2007.
- [5] British Standards Institute. Method of Testing Concrete, Part 2-Methods of Testing Fresh Concrete, BS 1881, Part 2:1970, London.
- [6] Cement Association of Canada, 2002, Design and Control of Concrete Mixture, Seventh Edition, Cement Association of Canada, Ottawa.
- [7] Chidiac S. E., Habibbeigi F., “Modeling the Rheological behaviour of fresh concrete: An elasto-viscosity finite element approach”, Computers and Concrete Journal, Vol. 2, No. 2, pp. 97-110, February 9, 2005.



- [8] Chidiac S. E., Habibbeigi F., Chan D., "Slump and Slump Flow for Characterizing Yield Value of Fresh Concrete", *ACI Materials Journal*, Issue.6, pp. 413-418, November 1, 2006.
- [9] Chidiac S. E., Maadani O., Razaqpur A.G., and Mailvaganam N.P., "Correlation of Rheological Properties to Durability and Strength of Hardened Concrete", *Journal of Materials in Civil Engineering*, V.1, Issue 4, pp. 391-399, July/August 2003.
- [10] Chidiac S. E., Maadani O., Razaqpur A. G., and Mailvaganam N. P., "Controlling the Quality of Fresh Concrete - A New Approach", *Magazine of Concrete Research*, V. 52, No. 5, Oct. 2000, pp. 353-363.
- [11] CSA test method A23.2-2A "Sieve Analysis of Fine and Coarse Aggregate" *Concrete Materials and Methods of Concrete Construction/Methods of Tests for Concrete*, 2000.
- [12] CSA test method A23.2-12A "Relative Density and Absorption of Coarse Aggregate" *Concrete Materials and Methods of Concrete Construction/Methods of Tests for Concrete*, 2000.
- [13] CSA test method A23.2-10A "Density of Aggregate" *Concrete Materials and Methods of Concrete Construction/Methods of Tests for Concrete*, 2000.
- [14] CSA test method A23.2-6A "Relative Density and Absorption of Fine Aggregate" *Concrete Materials and Methods of Concrete Construction/Methods of Tests for Concrete*, 2000.

- [15] CSA test method A23.2-9C "Compressive Strength of Cylindrical Concrete Specimens" Concrete Materials and Methods of Concrete Construction/Methods of Tests for Concrete, 2000.
- [16] CSA test method A23.2-4C "Air Content of Plastic Concrete by the Pressure Method" Concrete Materials and Methods of Concrete Construction/Methods of Tests for Concrete, 2000.
- [17] CSA test method A23.2-5C "Slump of Concrete" Concrete Materials and Methods of Concrete Construction/Methods of Tests for Concrete, 2000.
- [18] De Larrard F., "Why Rheology Matters", Concrete International (Concr. int.) ISSN 0162-4075, 1999, V. 21, pp. 79-81.
- [19] De Larrard F., C. Hu, T. Sedran, J. C. Sztikar, M. Joly, F. Claux, and F. Derkx, "A New Rheometer for Soft-to-Fluid Fresh Concrete", ACI Materials Journal, Issue.3 May 1, 1997, pp. 234-243.
- [20] Domone, P., "The Slump Flow Test for High-Workability Concrete," Cement and Concrete Research, V.28, No.2, 1998, pp. 177-182.
- [21] Ferraris C.F., "Measurement of the Rheological Properties of High Performance Concrete: State of Art Report", Journal of Research of the National Institute of Standard and Technology, 461-478, 1999.
- [22] Ferraris C. F and De Larrard F., "Testing and Modelling of Fresh Concrete Rheology", NISTIR 6094, Building and Fire Research Laboratory, National Institute of Standards and Technology, February 1998.
- [23] Ferraris C. F., and L. E. Brower, "Comparison of Concrete Rheometer: International Test at LCPC," National Institute of Standards and Technology, NISTIR 6819, 2000.

- [24] Ferraris C. F., and L. E. Brower, "Comparison of Concrete Rheometer: International Test at MB (Cleveland, Ohio) in May 2003," NISTIR 7154, Sep. 2004, 100 pp.
- [25] Hu C., F. de Larrard, and O. E. Gjorv, "Rheological Testing and Modeling of fresh High Performance Concrete", *Materials and Structure*, V.28, N.1, January, 1995, pp. 1-7.
- [26] Jang, J.-S.R., Sun, C.-T., 1995, Neuro-Fuzzy Modeling and Control, *Proceedings IEEE* 83 (3), 378-406.
- [27] Jang, J.-S.R., 1993, ANFIS: Adaptive-Network-Based Fuzzy Inference System, *IEEE Transactions on Systems, Man and Cybernetics*, 23(3), 665-685.
- [28] Kurokawa, Y.; Tanigawa, Y.; Mori, H.; and Komura, R., "A Study on Slump Tests and Slump-Flow Test of Fresh Concrete," *Transactions of the Japan Concrete Institute*, 16, 1994, pp. 25-32.
- [29] Koehler E. P., D. W. Fowler and C. F. Ferraris, "Summary of existing concrete workability test methods", *International Center for Aggregate Research*, The University of Texas, 2003.
- [30] Lydon F.D. "Concrete Mix Design", *Applied Science Publisher LTD* , England, 1972.
- [31] McIntosh J.D., 1966, "Concrete Mix Design", Second Edition, Published by the Cement and Concrete Association, London.
- [32] (Montgomery D.C. and Runger G.C., "Applied Statistics and Probability for Engineers", Third edition, 2003).

- [33] Mehta P.K., and P.J. Meterio, Concrete Structure, Properties, and Materials, Second Edition, Prentice-Hall, 1993.
- [34] Nayaka P.C., Sudheerb K.P., Ranganc D.M. and Ramasastrid K.S., 2004, "A Neuro-Fuzzy Computing Technique for Modeling Hydrological Time Series", Journal of Hydrology, 291, 52-66.
- [35] Takagi T., Sugeno, M., 1985, Fuzzy Identification of Systems and its Application to Modeling and Control, IEEE Transactions on Systems, Man and Cybernetics 15 (1), 116-132.
- [36] Tattersall G.H. and Banfill P.F.G., 1983, "The Rheology of Fresh Concrete", Pitman Publishing.
- [37] Tanigawa, Y., Mori, H., Kurokawa Y., and Komura, R., "Rheological study on slumping Behaviour of Fresh Concrete" Transactions of the Japan Concrete Institue, V.14, 1992, pp. 1-8.
- [38] Tanigawa, Y., Mori, H., "Rheological Analysis of Slumping Behaviour of Fresh Concrete," Proceeding of the 29th Japan Congress on Materials Research, 1985, pp. 129-136.
- [39] Xiong, L.H., Shamseldin, A.Y., O'Connor, K.M., 2001, A Nonlinear Combination of the Forecasts of Rainfall-Runoff Models by the First Order Takagi-Sugeno Fuzzy System, Journal of Hydrology 245 , 196-217.